

**SYNTHESIS, CHARACTERIZATION, AND ION EXCHANGE PROPERTIES
OF A SODIUM NONATITANATE, $\text{Na}_4\text{Ti}_9\text{O}_{20} \cdot x\text{H}_2\text{O}$**

A Thesis

by

GINA MARIE GRAZIANO

Submitted to the Office of Graduate Studies of
Texas A&M University
in partial fulfillment of the requirements for the degree of

MASTER OF SCIENCE

May 1998

Major Subject: Chemistry

SYNTHESIS, CHARACTERIZATION, AND ION EXCHANGE PROPERTIES
OF A SODIUM NONATITANATE, $\text{Na}_4\text{Ti}_9\text{O}_{20} \cdot x\text{H}_2\text{O}$

A Thesis

by

GINA MARIE GRAZIANO

Submitted to Texas A&M University
in partial fulfillment of the requirements
for the degree of

MASTER OF SCIENCE


Approved as to style and content by:



Abraham Clearfield
(Chair of Committee)



Victoria J. DeRose
(Member)



Lloyd R. Hossner
(Member)



Emile A. Schweikert
(Head of Department)

May 1998

Major Subject: Chemistry

ABSTRACT

Synthesis, Characterization, and Ion Exchange Properties of a Sodium Nonatitanate,

$\text{Na}_4\text{Ti}_9\text{O}_{20} \cdot x\text{H}_2\text{O}$. (May 1998)

Gina Marie Graziano, B.S., Rensselaer Polytechnic Institute

Chair of Advisory Committee: Dr. Abraham Clearfield

During the Cold War, the Hanford Weapons Site in Richland, Washington, produced weapons grade plutonium which first needed to be separated from the other products using the PUREX process (plutonium and uranium extraction). As a by-product of this process, millions of cubic meters of highly acidic radioactive waste were produced which are now stored in million gallon tanks at the Hanford site. Over the years, some tanks have been known to leak and some are even in danger of exploding. Because of these problems, the waste needs to be removed from these tanks and given permanent, safe storage. The purpose of this research is to produce a more efficient ion exchanger to separate the highly radioactive isotopes (^{90}Sr , ^{137}Cs and transuranics) from the large quantities of inert salts. The smaller volume of high level waste produced can then be vitrified in glass and stored, while the low level waste can be poured into less expensive cement and glass.

In this work, different parameters of the synthesis of the sodium nonatitanate ion exchanger, $\text{Na}_4\text{Ti}_9\text{O}_{20} \cdot x\text{H}_2\text{O}$, such as the Na and Ti reactants, the heating time, oven temperature, Na:Ti mole ratio, and heating method, were altered and their effects on Sr^{2+} ion exchange selectivity were examined. For example, the heating time was varied from

1 day to 2, 3, 7, and 30 days. Although the crystallinity remained the same from the 1 day to the 2 day sample, as the heating time further increased, the crystallinity improved. The most Sr selective material was the 2 day sample with a K_d (distribution coefficient) of 1.22×10^6 ml/g in 0.1M Na/ 0.001M Sr solution. The K_d 's steadily decreased as the sample crystallinity increased with a maximum K_d of only 1.60×10^5 in 0.01M Na/ 0.001M Sr solution after a heating time of 30 days. However, in a simulated waste such as NCAW, the 2 day sample gave a K_d of only 1.44×10^5 ml/g, while the 1 day sample gave a value of 2.50×10^5 . This indicates that the nonatitanate synthesis needs to be uniquely designed to optimize Sr^{2+} removal in each specific type of waste to be remediated.

DEDICATION

To my parents, Anthony and Patricia, and my sisters, Patty and Barbara, for their unending love and support. Without them, nothing would be possible.

ACKNOWLEDGMENTS

I would like to thank my advisor, Dr. Abraham Clearfield, for providing me the opportunity to work for him and for being so helpful and understanding of my circumstances. I would also like to thank the members of the Clearfield group, especially Deirdre Arnold, Rick Carroll, Daniel Grohol, Boris Shpeizer, and Baolong Zhang, for always offering a much needed hand, and friendly words of conversation. I especially thank our secretary, Judy Angel, for her helpful advice, many entertaining talks, and friendship which made every day more enjoyable.

Finally, I would like to give a very special thanks to Elizabeth Behrens and Paul Sylvester. I can't find the words to express how grateful I am to them for being such good friends and for taking so much time out of their day to teach me, answer my many questions, and guide me in my research. Without them, this research and thesis would not have been possible.

TABLE OF CONTENTS

	Page
ABSTRACT	iii
DEDICATION	v
ACKNOWLEDGMENTS	vi
TABLE OF CONTENTS	vii
LIST OF FIGURES	viii
LIST OF TABLES	x
 CHAPTER	
I INTRODUCTION	1
History	1
Past Research	6
II SYNTHESIS	19
Synthesis of Sodium Nonatitanate	19
Synthesis Variations	23
Variations in the Synthesis Reactants	33
III ION EXCHANGE PROPERTIES	44
K _d Determinations	44
Waste Simulant Batch Tests	62
pH Batch Tests	66
Column Tests	67
Industrial Testing	71
IV CONCLUSIONS	74
REFERENCES	79
APPENDIX A	82
VITA	87

LIST OF FIGURES

Figure	Page
1.1 Diagram of the Na titanasilicate, $\text{Na}_2\text{Ti}_2\text{O}_3\text{SiO}_4 \cdot 2\text{H}_2\text{O}$	10
1.2 Representation of a. $\text{Na}_2\text{Ti}_3\text{O}_7$, and b. $\text{K}_2\text{Ti}_4\text{O}_9$	15
2.1 XRD pattern of GMG-I-1, the Na titanate sample synthesized with the original parameters	20
2.2 Thermogravimetric analysis (TGA) of GMG-I-1	21
2.3 Scanning electron micrograph of GMG-I-1 at a magnification of 5000x	22
2.4 XRD pattern of the titanate synthesis with oven time variations. a. GMG-I-1 (1 day), b. GMG-I-10a (2 days), c. GMG-I-10b (3 days), d. GMG-I-10c (7 days), e. GMG-I-10d (30 days).....	25
2.5 Thermogravimetric analysis (TGA) of GMG-I-10d	27
2.6 Scanning electron micrograph of GMG-I-10d at a magnification of 1000x	28
2.7 XRD pattern of the titanate synthesis with oven temperature variations. a. GMG-I-22a (150°C, scale x10), b. GMG-I-22b (170°C), c. GMG-I-1 (200°C, scale x10).	30
2.8 XRD pattern of the titanate synthesis with heating method variations. a. GMG-I-28 (w/o bomb), b. GMG-I-27 (w/o preheating), c. GMG-I-1 (original), d. GMG-I-39 (slow quenching).....	32
2.9 XRD pattern of GMG-I-34, Sr titanate synthesis where SrTiO_3 (closed arrows) formed with $\text{Na}_4\text{Ti}_9\text{O}_{20}$ (open arrows)	37
2.10 XRD pattern of the SrTiO_3 synthesis, a. GMG-I-38b1 (300°C), b. GMG-I-38b2 (500°C). The arrows indicate where SrTiO_3 peaks began to emerge.....	38
2.11 XRD pattern of the Cs titanate synthesis. a. GMG-I-43 (Cs titanate before washing), b. GMG-I-43a1 (after NaCl wash), c. GMG-I-43b (after Na_4EDTA wash)	40

LIST OF FIGURES (CONTINUED)

Figure	Page
2.12 XRD pattern of GMG-I-55, the K titanate synthesis, which shows a mixture of $K_2Ti_6O_{13}$ and $K_2Ti_8O_{17}$	41
2.13 XRD pattern of GMG-I-57, the Nb doped sample. The arrow points to a possible Nb peak.....	43
3.1 K_d graph assessing the ion exchange selectivity of GMG-I-1 for alkaline earth metals.....	46
3.2 K_d graphs of the heating time variation series, samples GMG-I-1 & 10a-d in a. Na/Sr, b. Mg/Sr, c. Ca/Sr, and d. Ba/Sr solutions.....	48
3.3 K_d graphs of the temperature variation series, samples GMG-I-1, 22a, & 22b in a. Na/Sr, b. Mg/Sr, c. Ca/Sr, and d. Ba/Sr solutions.....	51
3.4 K_d graphs of the Na:Ti mole ratio variation series, samples GMG-I-1, 24a, 24b, & 24c in a. Na/Sr, b. Mg/Sr, c. Ca/Sr, and d. Ba/Sr solutions.....	55
3.5 K_d graphs of the heating method variation series, samples GMG-I-1, 27, 28 & 39 in a. Na/Sr, b. Mg/Sr, c. Ca/Sr, and d. Ba/Sr solutions.....	58
3.6 Sr column data for GMG-I-1 inorganic beads in NCAW simulant.....	68
3.7 Sr column data for GMG-I-1 organic beads in NCAW simulant.....	69
3.8 Sr exchange kinetic study on GMG-I-1 inorganic beads.....	70
3.9 Sr column data for GMG-I-1 inorganic beads in 101SY simulant.....	72
3.10 Sr column data for GMG-I-59 inorganic beads in 101SY simulant.....	72

LIST OF TABLES

Table	Page
2.1 Summary of changes in the titanate synthesis method.	24
2.2 Summary of changes in the reactants used for titanate syntheses.....	34
3.1 Comparison of K_d values for GMG-I-1 and GMG-I-59 in Na/Sr, Mg/Sr, Ca/Sr and Ba/Sr solutions.....	61
3.2 Compositions of tank waste simulants, NCAW, 101SY-Cs5, and N- Springs, courtesy of G. N. Brown of Pacific Northwest National Laboratory.....	63
3.3 Sr K_d values for samples GMG-I-1-10d in NCAW waste simulant.....	64
3.4 Cs K_d values for all titanate samples in N-Springs waste simulant.....	65
3.5 Comparison of Sr K_d values for various exchangers in KE-Basin water using a volume : mass ratio of 10^4	73

CHAPTER I

INTRODUCTION

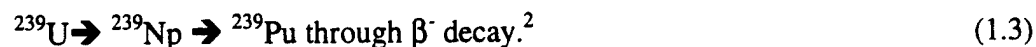
History

In the early 1900's, Hahn and Strassmann found that uranium, which is naturally found within the earth as ^{238}U (99.274%), ^{235}U (0.7205%) and ^{234}U (0.0056%)¹, was fissionable. This meant that not only would the element naturally decay, but also when bombarded with neutrons¹ according to the following equation,



Researchers realized the fact that each neutron produced could be reacted with another ^{235}U to form a chain reaction, resulting in the release of an enormous amount of energy. This release of energy results from conversion of a small amount of mass to energy according to the mass-energy law $E=mc^2$, allowing nuclear fission to be used in weapons and power production.

In the case of nuclear power, this reaction would be slowed, cooled, and controlled in order to produce a steady flow of energy. However, in the case of nuclear weapons, the reaction would be continued with fertile ^{238}U which undergoes the following reaction in a nuclear reactor,



This thesis follows the style and format of *Journal of the American Chemical Society*.

The ^{239}Pu produced can be used in nuclear weapons where its fission would be allowed to proceed in an uncontrolled manner generating enough energy to produce a nuclear explosion. However, the Pu had to be separated out from the irradiated fuel first, primarily by using the PUREX process (plutonium and uranium extraction) as well as other less common methods such as the bismuth phosphate process³. In the PUREX process, first the irradiated fuel rods are dissolved in nitric acid then contacted with a solution of tri-n-butylphosphate (TBP) dissolved in kerosene or carbon tetrachloride. The uranium and plutonium are complexed by TBP and extracted into the organic phase, leaving the fission products in the aqueous phase. The organic phase is then mixed with an aqueous solution containing a reducing agent such as Fe(II) amidosulphate. Pu(IV) is reduced to Pu(III) which, because of its properties, is no longer complexed by the TBP and is extracted into the aqueous phase while the stable U(VI) is not reduced and remains complexed with the TBP. The remaining uranium in the organic phase is then contacted with water or dilute nitric acid and is extracted out into the aqueous phase.² Over the years, an enormous amount of highly acidic liquid waste has been produced from each of these processes. There are 5.5 million cubic meters stored, containing 31 billion curies of radioactivity.⁴

Specifically, this thesis concentrates on the Hanford Weapons Site located in Richland, Washington, where most of the weapons grade plutonium production during the Cold War occurred.⁵ In Hanford, since the start of plutonium production in 1943, high level waste (HLW), which the Department of Energy defines as any highly reactive waste needing "permanent isolation"⁴, from the PUREX and other processes, has been

deposited into million gallon volume storage tanks. The workers also added into these tanks various other mixtures of chemicals including fission products, various solvents, and other wastes from clean up attempts.³ As a result of these actions, each of the tanks contains a variety of different chemicals which changes from one tank to another. For example, in tank 241-AN-107, some of the more abundant species include Al, Ca, Cr, Fe, K, Na, Ni, U, and Pu, along with a range of anions including NO_3^- , NO_2^- , PO_4^{3-} , SO_4^{2-} , acetate, EDTA, formate, glycolate, HEDTA, and various hydrocarbons.⁶ Surveys from Battelle Pacific Northwest National Laboratory show that tank 101SY includes numerous complexants such as EDTA, HEDTA, citric acid, iminodiacetic acid, and Na-gluconate which chelate many radioactive metals such as ^{90}Sr , making them difficult to extract through ion exchange. In another example, the Neutralized Current Acid Waste tank (NCAW), #241-AZ-102, includes over 200 g/L Na^+ and over 150 g/L Al^{3+} .

Most of the wastes were very acidic and once they were deposited into the tanks, the pH was raised to 13 or greater using NaOH so the waste would not degrade the steel tank lining.^{7,8} This process resulted in the formation of a 7-8 M, or greater, NaNO_3 solution causing a salt cake layer to form at the top of the tank. The transition and actinide metals precipitated out as hydroxides and formed a sludge layer at the bottom of the tank. When the organic materials between these layers decompose, they produce hydrogen and other gases which end up being trapped between the solid masses giving rise to a pressure build up and a possible violent explosion. This would result in the scattering of radioactive waste into the atmosphere and surrounding area.^{7,8}

In all, 177 tanks were used to store this waste, 149 of which are single-shell lined while 28 are double shelled. Waste has leaked from some of the single shelled tanks (SST) and has come out of underground drainage cribs where lower level waste was stored.⁷ As a result, the soil was contaminated with radioactivity, heavy metals, and organics, some of which has reached the ground water supplies. Hanford estimates that over 500 km² of soil was contaminated.⁵ Researchers have tried several methods to remediate the soil and water and only bioremediation, a process where microbes breakdown the waste for their energy production, seems to be effective.^{5,8} The problem is that this process is very slow and the microbes can only degrade organic waste. Scientists are working toward making their own microbes that can "eat" faster.

Another solution to the soil contamination problem is "in situ" vitrification where electrodes are placed within the ground and a high current is passed through them. This melts the soil causing it to form into a stable glass on cooling.^{8,9} The contaminated soil is thus encapsulated, preventing any radionuclides or heavy metals from migrating down into the ground water. The advantage of locking this soil right in place, is that it eliminates the need for workers to dig the soil out, and thus reduces any further environmental hazards.⁸

Because these tanks are posing so many problems between leaking, dangerous mixtures of different wastes, and possible explosions, they are not suitable for continued waste storage. The contents now need to be removed and given permanent disposal.

A solution that is being developed for this problem is separation and vitrification. The process involves first separating the waste according to their differing levels of

activity. Once the high level waste, containing mostly ^{90}Sr , ^{137}Cs , and transuranics, is extracted, the remaining inert salts and organics can be classified as low level waste (LLW). The high level wastes are then mixed with ground glass and heated together at about 1100°C after which it is poured into steel canisters and allowed to solidify into a stable form.⁵ The LLW can also be made into glass or mixed with cement in steel drums and stored safely. The problem is that vitrification is expensive and the key is for the waste to be efficiently separated, i.e. to pull out all the long lived isotopes completely, minimizing any inert materials mixed within. This would reduce the volume needed for the expensive HLW vitrification⁵ and enable the LLW to be safely stored in glass or cement which is much less expensive due to lower shielding requirements.⁷ Once in these glass encasements, the waste is temporarily stored prior to its permanent disposal.

Plans have already begun for permanent storage sites, one is called the Waste Isolation Pilot Plant (WIPP) in Pecos Valley, New Mexico.⁹ The reason for choosing this site is because it is a salt valley, which means the area is dry and stable. There is little chance of a catastrophic occurrence and even if there was, there is little chance of any waste finding its way to a water source.^{9,10} It is planned to store 6 million ft^3 of transuranic (TRU) waste, (i.e. elements with a greater atomic number than uranium), 650 meters under this valley. Considering all the possible problems that may occur, the WIPP site seems to be able to maintain its safety into the future;⁹ although, an article by North¹⁰ mentions a possible threat from human disturbance due to potential oil drilling in that area.

Another projected site is at Yucca Mountain in southwestern Nevada.⁹ This is also another dry area, lowering the possibility of water contamination.¹⁰ It is planned to store 70,000 tons of spent fuel rods and 8,000 tons of the vitrified HLW canisters 300 meters below the Yucca Mountain surface. The engineers also plan to put an additional barrier around the canisters within the site to prevent migration of radionuclides into the surrounding area. However, there are a lot of factors that are just too difficult to predict, such as corrosion of the canisters due to the geological environment or even human behavior¹⁰ which make it difficult to say whether or not the Yucca site will remain safe far into the future.⁹

Past Research

This report focuses on the process of more efficiently separating out the HLW in the Hanford tanks which would reduce the high activity waste volumes and hence the overall costs of their solidification and disposal. Most of the research has been focused on the separation of ^{137}Cs and ^{90}Sr , (the most abundant radioactive isotopes found in the liquid phase), from the rest of the tank waste materials.

Some organic materials have been examined for their ability to extract radioactive ions from solution. One such material is the DiphonixTM Resin which is a styrenic based polymer with appended diphosphonic acid and sulfonic acid groups.¹¹ It was found through a comparison of Group II metal uptake with a diphosphonic acid resin and a sulfonic acid resin, that the Diphonix Resin performed similarly to the phosphonic acid resin. This led to the conclusion that in the Diphonix Resin, it was the phosphoric

acid group that ligated to the metal first until it was saturated, at which time the sulfonic acid would begin to take up the metal. As for the specific uptake of the Group II metals by the Diphonix Resin, there was no selectivity based on metal size as with other exchangers. The Diphonix Resin loses 2H^+ ions from 2(POH) groups which enables the oxygens to chelate to the metal; it is this chelating ability that decides the metal uptake. Through Infrared Spectroscopy, it was found that the Diphonix POH absorption bands were not altered after Group II metal chelation, indicating that more of an ionic bond was formed.¹¹ Nonetheless, this resin seems to provide an option for separating radioactive ions from solution.

Crown ethers in a variety of different diluents have also been looked at for use in nuclear waste remediation due to their ability to act as a polydentate ligand and chelate metals. Horwitz, et al.¹² found the best Sr extraction, (SrEX), results were produced from using di-t-butylcyclohexano-18-crown-6 (DtBuCH18C6) in 1-octanol. Through experiments using 0.2 M crown ether with increasing concentrations of HNO_3 in a simulated sludge waste containing primarily 1.3×10^{-3} M radioactive Sr, 6.6×10^{-5} M radioactive Ba, 0.15 M Na, 0.0014 M Ca, and 0.046 M Al, it was found that the crown ether was able to extract Sr efficiently over Na and Ca even as the concentration of HNO_3 increased; although, Ba seemed to pose some uptake competition. It was also noticed that as the radioactivity level of the waste solutions is increased, the crown ether begins to break apart into short chains, thus limiting its use as a long term storage option.¹² This seems to be the case for most organic ligands; thus, inorganic materials were looked toward due to their high stability.

For many years, zeolites have been used as ion exchangers within the nuclear industry. Zeolites are aluminosilicate structures with repeating units and are ordered such that pores are formed where exchangeable ions are bound.¹³ There are different types of zeolites giving different pore sizes. When the pore size matches the size of an ion, that zeolite will be an effective ion exchanger for that ion. Two zeolites, synthetic mordenite, Zeolon 900, and synthetic chabazite, Linde AW-500, were looked at for ¹³⁷Cs ion exchange from waste solutions from the Loviisa Nuclear Power Plant in Finland.¹³ The waste solutions included one with a low salt concentration of Na⁺ ions (8-21 mmol/L) and K⁺ ions (0.5-7.0 mmol/L) and another with a high salt concentration of Na⁺ (2.7 mol/L) and K⁺ (.24 mol/L). K_d batch tests were performed where each zeolite was mixed with the low salt waste solution. K_d is the distribution coefficient, a measure of ion exchange ability where

$$K_d = [(C_I - C_F) / C_F] \times (V/m) \quad (1.4)$$

C_I and C_F are the initial and final Cs⁺ concentrations, respectively and V is the solution volume (ml) and m is the exchanger mass (g). It was found that increasing concentrations of Na⁺ and K⁺ in the waste solutions lowered the effectiveness of the Cs⁺ uptake by competing for available exchange sites. Potassium ions were more of a hindrance because their size is closer to Cs⁺. In experiments where the waste solutions were passed through columns containing each zeolite, only 42% of the total Cs⁺ was absorbed into AW-500 and 62% absorbed into Zeolon 900 using the high salt waste. However, in the low salt solution where there were fewer competing ions, 95% of the Cs⁺ was absorbed onto both zeolites. In all tests, both zeolites performed approximately

equally.¹³ From this, it can be concluded that in solutions with large concentrations of alkali cations, these zeolites aren't very effective for Cs^+ separation.

In the accident at 3 Mile Island, highly active waste (100 Ci/m^3) was produced from coolant water and spillage. The water contained mostly ^{90}Sr and ^{137}Cs along with ~2000 ppm B and 1600 ppm Na. A series of columns were set up within a spent fuel pool using a 3:2 ratio mixture of zeolites IE-96 and A-51 for optimal removal of both Cs^+ and Sr^{2+} .¹⁴ After ~2000 bed volumes of the water was flushed through the first column, it was removed and the others were advanced forward one position. This process was continued until all of the water cycled through in order to allow for maximum contact time with the exchanger to ensure complete purification. Approximately 10 columns, which were used as the permanent storage containers, were needed to decontaminate all the waste.¹⁴

In a study by Kanno¹⁵, a series of zeolites were studied for Cs^+ uptake in High Level Liquid Waste (HLLW) solutions. Synthetic and natural mordenite, clinoptilolites, and A, X, and Y zeolites were looked at. They found that synthetic mordenite has one pore type that will exchange for Cs^+ . However, zeolite A for example, has 2 pore types and only one will exchange for Cs^+ . Mordenite had a higher selectivity in this case and was the most efficient in Cs^+ uptake. Heating the Cs-mordenite to $>1000^\circ\text{C}$ formed a stable ceramic permanently trapping the Cs^+ within. In this study, mordenite seems to be the zeolite of choice for Cs^+ .¹⁵

Another type of material that was investigated for its ion exchanging ability was sodium titanosilicate, $\text{Na}_2\text{Ti}_2\text{O}_3\text{SiO}_4 \cdot 2\text{H}_2\text{O}$, the structure of which is given in Figure 1.1.

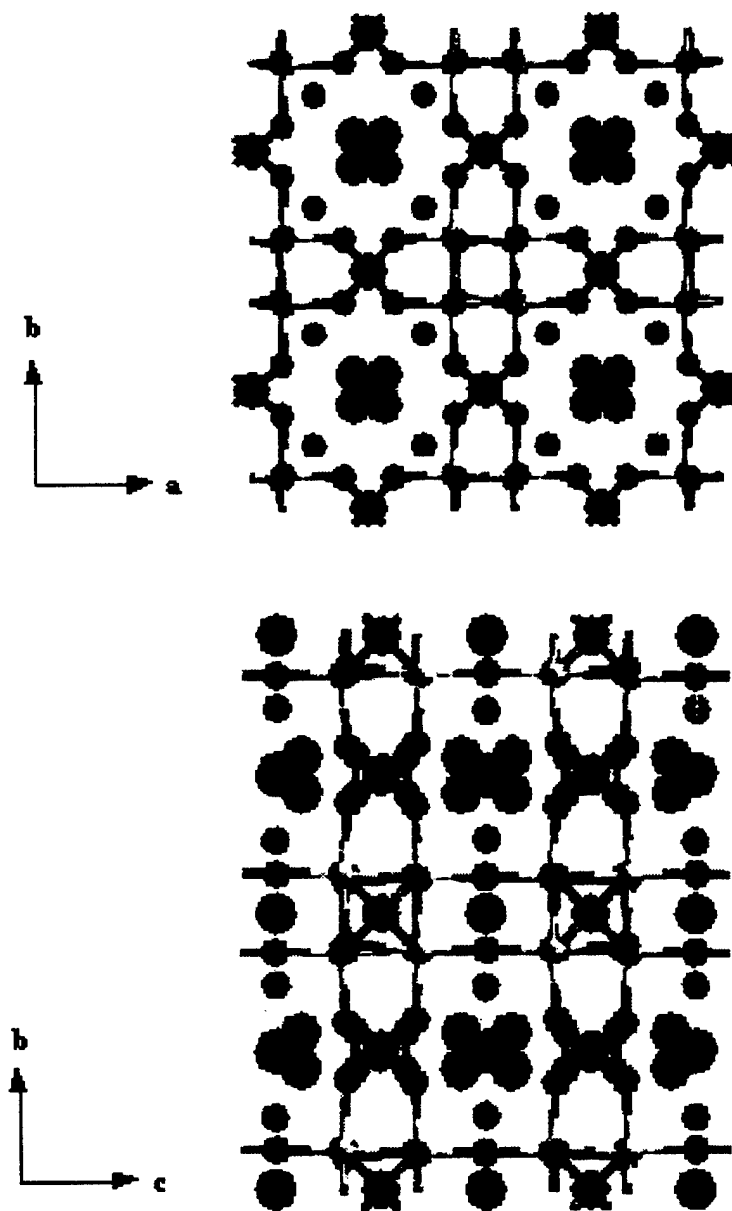


Figure 1.1. Diagram of the Na titanosilicate, $\text{Na}_2\text{Ti}_2\text{O}_3\text{SiO}_4 \cdot 2\text{H}_2\text{O}$.

In this compound, the Ti atoms are arranged in a box formation with 2 Ti atoms at opposite corners on the bottom and 2 more rotated by 90° at the alternate corners on top. Each Ti atom is octahedrally coordinated to the oxygens to form TiO_6 . These clusters of 4 Ti octahedra are located at the corners of a tetragonal unit cell and at the edges half-way along the c axis and are bridged to each other along the a and b axis by silicate groups and along the c axis by oxo groups. There are two types of Na^+ ions, one set binds to the SiO_4 oxygens as well as to H_2O oxygens. These Na^+ ions are held within the framework and won't exchange with Cs^+ . The other type of Na^+ ions are exchangeable and are found within the tunnels created by the structure. Because Na^+ ions can not fill all of these sites due to their size, H^+ ions fill the remaining sites in order to maintain the overall charge resulting in the true formula $\text{Na}_{1.64}\text{H}_{0.36}\text{Ti}_2\text{O}_3(\text{SiO}_4) \cdot 1.84\text{H}_2\text{O}$.¹⁶

When Na^+ ions within the tunnels exchange for Cs^+ , a much better fit is found. The Na^+ ions, because of their smaller size, create a distorted bonding arrangement when attempting to bond to each oxygen. Cs^+ is larger and by locating in the center of the tunnels at the level of the Si atoms, can bond to the oxygens equally, so it creates more favorable Cs-O bond lengths and is therefore the more favored ion. However, because of its size, crowding occurs with Cs^+ and prevents complete exchange for all exchangeable Na^+ ions.¹⁶

Further tests were done to examine the Cs^+ uptake ability of the sodium titanosilicate.¹⁷ The material was changed into the H-form, and Na^+ and Cs^+ uptake were looked at separately. As the pH increased, Na^+ uptake increased while Cs^+ uptake hardly changed; however, overall Cs^+ uptake was better in the H-form because of less crowding

from Na^+ ions. This prompted a look at what Cs^+ uptake would be like when competing with Na^+ . When the H-form of the silicate was placed in a Cs^+ and Na^+ solution, the Cs^+ uptake remained low and constant as the pH was raised, while Na^+ uptake sharply increased. When the Na^+ form was in a .001M Cs^+ solution at high pH, the Cs^+ uptake drastically decreased as Na^+ concentration increased. Even though Cs^+ fits better into the titanosilicate structure, when competing with Na^+ , the Na^+ ions just seem to exchange faster and block the Cs^+ ions.¹⁷ This is unfortunate because the tank wastes are highly alkaline with large Na^+ concentrations. So it appears that the titanosilicate, while very selective for Cs^+ , has a low Cs^+ capacity.

Another type of titanosilicate, $\text{HM}_3\text{Ti}_4\text{O}_4(\text{SiO}_4)_3 \cdot \text{H}_2\text{O}$ where $\text{M} = \text{H}^+, \text{K}^+, \text{Cs}^+$, which is structurally comparable to the pharmacosiderite mineral, was studied by Behrens, et al.¹⁸ Its structure is similar to the Na titanosilicate previously mentioned in that it also contains TiO_6 octahedral units with the Ti atoms in the corners of a box formation; however, these clusters form the corners of a cubic structure as opposed to a tetragonal one. Together with SiO_4 tetrahedra bound between these clusters and protons bound to the oxygens connecting the Ti atoms, this structure produces cavities filled with H_2O in the H-form. However, 3 of the protons can exchange metal cations which will bind to the oxygens within the cavities along the cubic face centers. Ion exchange selectivity is highest for larger cations such as Cs^+ and Sr^{2+} as they will provide a better fit and form stronger bonds within the pores. This material is more effective at radioactive waste treatment than the previously mentioned titanosilicate because its cubic

structure allows ions to enter from every face providing more opportunity for radioactive ions to be locked within.¹⁸

In 1991, a transition metal hexacyanoferrate was marketed by Selion, under the name CsTreat™, to remove Cs⁺ from waste solutions.^{19,20} The mechanism of Cs⁺ exchange in hexacyanoferrates is still not fully understood; however, it has been found to be highly selective for Cs⁺, even in high salt concentrations. One liter of CsTreat was able to extract the Cs⁺ from over 8,000 L of a high salt waste solution from evaporator concentrates containing 40-70 g/L Na⁺ and 2-10 g/L K⁺. In a low salt solution from Naval reactors in Estonia, 1L of CsTreat processed over 63,000 L without even reaching its Cs⁺ exchange capacity at 1% breakthrough.¹⁹

In comparison with other exchangers such as the zeolite mordenite, CsTreat proved to be far more efficient.^{19,20} The zeolite is often blocked by such ions as Na⁺ and K⁺, while the hexacyanoferrate is not. It was noted however, that CsTreat efficiency was hindered by very high K⁺ concentrations (about .2 M) and by high pH levels (>13) where it dissolves. The issue of a selective ion exchanger becomes so important because as the long lived isotopes (HLW) can be more efficiently separated away from the inert salts, less volume is produced that needs to be vitrified by expensive means. This means that less storage space will be needed for the canisters, and less money will be spent.²⁰ The rest of the low level liquid waste can be safely stored by less expensive means. It is because of this selectivity that CsTreat and other selective exchangers have become so useful; although, CsTreat is not suitable for storage purposes.

The research presented in this study concentrates on a sodium titanate ion exchanger which exhibits a high selectivity for Sr^{2+} or $\text{Sr}(\text{OH})^+$ in solutions of high alkali and alkaline earth ion concentrations. In the late 70's, a new class of compounds of the general formula $\text{M}[\text{M}'_x\text{O}_y\text{H}_z]_n$, where M is an alkali metal (Na^+ , K^+) and M' is a tetravalent metal (Ti, Zr...), was found to be effective in nuclear waste remediation. The $\text{HNaTi}_2\text{O}_5 \cdot x\text{H}_2\text{O}$ form seemed to be the most effective for ion exchange.²¹ In a waste containing ^{90}Sr , the Na^+ and Sr^{2+} ions would exchange, after which vitrification can be used to lock the radioactive Sr^{2+} within the solid for permanent storage. The other abundant radioactive ion in nuclear waste is ^{137}Cs . Since the titanate prefers to exchange with divalent ions, it wasn't as effective with Cs^+ exchange as it was with Sr^{2+} . It was noted that by lowering the pH, the hydrogen form $\text{H}_2\text{Ti}_2\text{O}_5 \cdot x\text{H}_2\text{O}$ is produced which hinders ion exchange due to the affinity of the titanate for the H-form.²¹

"Titanates" of the form $\text{M}_2\text{Ti}_n\text{O}_{2n+1}$ have been looked at, specifically $\text{Na}_2\text{Ti}_3\text{O}_7$ and $\text{K}_2\text{Ti}_4\text{O}_9$ were analyzed for their ion exchange ability.²² The two structures, see Figure 1.2, are similar to each other with TiO_6 octahedra linked together across the x and z directions. In the Na compound, Na^+ ions are found between each layer at 2 different sites. The K^+ ions are located at one site in every other layer, where the empty layers are almost compressed.

Each of these two compounds was mixed with HCl, then examined by X-ray data to determine if H^+ ions were exchanged for Na^+ and K^+ . The interlayer distance of the Na compound was found to compress, which was due to the smaller H^+ ions exchanging for the larger Na^+ ions.²² The interlayer distance of the K compound was found to

increase. This is because if an ion as small as H^+ exchanged with K^+ in this particular structure where every other layer is nearly compressed, the layers would get too close. H_3O^+ , which is larger than K^+ , is exchanged into the layers instead in order to keep them apart. These materials were then mixed with $NaCl/NaOH$ and KCl/KOH solutions respectively. Through similar means of using X-ray data to watch the interlayer distances change, it was found that the original ion exchanged back into the structure.²² According to this data, these titanates seem to be effective at exchanging their natural cations for H^+ .

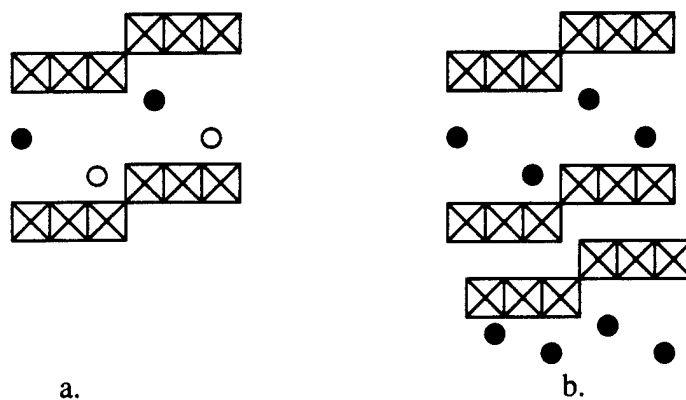


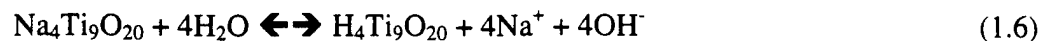
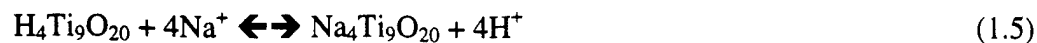
Figure 1.2. Representation of a. $Na_2Ti_3O_7$, and b. $K_2Ti_4O_9$.

As in the above procedure, when $K_2Ti_4O_9$ was mixed with HCl , a “hydrous titanium dioxide” was formed which was looked at for its ion exchanging ability and use in nuclear waste separation.^{23,24} In duplicate experimental trials where 2 g of the

hydrous titanium dioxide were mixed with a solution of $.03 \text{ mol dm}^{-3} \text{ Sr(OH)}_2$, the titanium dioxide was found to exchange its H^+ ions to form two allegedly distinct products, $\text{SrTi}_6\text{O}_{13} \cdot 6.7\text{H}_2\text{O}$ in one sample and $\text{SrTi}_4\text{O}_9 \cdot 6.7\text{H}_2\text{O}$ in the other sample. These materials were then heated to 1000°C to form a stable SrTiO_3 compound.²⁴ This seems to provide an effective remediation procedure.

Clearfield et al.²⁵ studied the titanate $\text{Na}_4\text{Ti}_n\text{O}_{2n+2}$, specifically $\text{Na}_4\text{Ti}_9\text{O}_{20} \cdot x\text{H}_2\text{O}$. The first peak of its X-ray pattern was found to vary from 10 to 6.9 \AA depending on the water content. They found that a dry sample gave a first peak at 6.9 \AA while a hydrated sample had a first peak at 10 \AA . Since the first peak usually represents the largest spacing within the structure and it changed with water content, they concluded that they had a layered compound and the water was wedging the layers apart. Theory also suggested that the layers consisted of TiO_6 connecting octahedral units with Na^+ ions between the layers, much like the sodium titanate described by Izawa et al.²² When these titanates were hydrothermally heated at $200\text{-}300^\circ\text{C}$, they came out crystalline and needle shaped. It was noted that as the temperature was lowered, a more amorphous powder was formed.²⁵

In further studies, it was found that the nonatitanates prefer to be in the hydrogen form $\text{H}_4\text{Ti}_9\text{O}_{20}$, so when in the Na form, exchange ability for Sr^{2+} is improved as the compound would rather exchange the Na^+ ions. The more the titanate exchanges, the more Na^+ ions are produced and the more basic the solution becomes causing an equilibrium shift towards the left where it will produce more of the Na-form of the titanate as shown in equations 1.5 and 1.6:



The Na-form promotes further exchange until a point is reached where there are too many Na^+ ions which then begin to compete for exchange sites, reducing the exchange capacity for Sr^{2+} .²⁶

Lehto et al.²⁷ reported on batch tests of this titanate. They shook a radioactive Sr^{2+} solution with the material, filtered the mixture, and tested the solution for residual radioactivity. They saw that the K_d values, the distribution coefficient, decreased as the Na^+ ion concentration in the solution increased. The best K_d was 5×10^4 ml/g at a Na^+ concentration of $<10^{-3}$ M. They also did tests where a solution of 0.01 M Sr^{2+} at pH 5 with a ^{85}Sr tracer was passed through a column containing the titanate. When the collected solution was at 50% of the initial solution's activity, the titanate was found to have a capacity of 3.4 meq Sr/g at a flow rate of 0.1 mL/min.²⁷

In the work for his Dissertation, Cahill²⁸ looked at three different synthesis methods for the sodium nonatitanate. The first method involved mixing Ti isopropoxide ($\text{Ti}(\text{OPr})_4$) with varying concentrations of NaOH in water, refluxing, and finally heating the mixture in a hydrothermal bomb at $\sim 200^\circ\text{C}$ for ~ 1 day. The second synthesis was similar to the first but excluded the refluxing step. The third synthesis was comparable to the second, using methanol media to form a gel rather than aqueous media. As the second synthesis didn't provide any new data and the third gave poor results, the first method was focused on.

It was noticed in the original synthesis that as the Na:Ti mole ratio increased, the material's crystallinity also increased until a ratio of 6.8 was reached where a possible second form of the titanate was produced with less crystallinity. As the mole ratio was further increased to 10, a third form of the material was produced. It was found that the mole ratio was the main factor that decided the crystallinity of the material, which in turn decided the Sr^{2+} ion selectivity. The more amorphous the product was, the better its selectivity became for Sr^{2+} , Ca^{2+} , and Li^+ . The titanate's preference for ions of such drastic size differences led to the conclusion that there are two different ion exchange sites within the material's layers.²⁸ Through this work, a better understanding of the titanate properties was achieved.

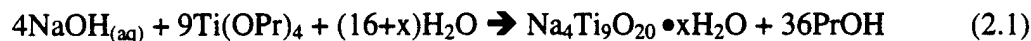
This research continues the experimentation on the synthesis of the sodium nonatitanate. The purpose of the work is to try to optimize the ion exchanging ability of the compound by altering its structure through synthesis. By producing a more efficient material, better separation of the ^{90}Sr in HLW can be achieved. This will lead to reduced waste volumes needed to be vitrified and stored, thereby meeting the goal of this waste problem.

CHAPTER II

SYNTHESIS

Synthesis of Sodium Nonatitanate

Sodium Nonatitanate, $\text{Na}_4\text{Ti}_9\text{O}_{20} \cdot x\text{H}_2\text{O}$, was prepared according to the method developed by Roy Cahill²⁸ which consists of adding 8.4 g of a 50% NaOH solution dropwise to 7.7 g of Ti isopropoxide, $(\text{Ti}(\text{OPr})_4)$, Aldrich 97%, in a Teflon round bottom flask while mixing and heating at 110°C for one hour. The mixture was stirred and heated at 110°C for three more hours and the contents were then transferred to a Teflon lined hydrothermal bomb with 12.8 ml of deionized water where it was heated at 200°C for one day. The bomb was then placed under tap water and quickly cooled in order to quench the reaction. The contents were filtered, washed with 200 ml of ethanol and placed in an oven at 85°C to dry for two days and the resulting product was designated GMG-I-1. This synthesis can be represented by the following equation:



The X-ray pattern of this solid product (and all other materials) was taken on a Rigaku RU 200 automated powder diffractometer at 50 kV and 180 mA (rotating anode) using $\text{Cu K}\alpha$ radiation and showed peaks at 9.83, 3.68, 3.12, and 1.89 Å, see Figure 2.1. These peaks were very broad and undefined indicating the material was poorly crystalline. The thermogravimetric analysis (TGA), taken using a Dupont Instruments 951 TGA, showed a graph with a weight decrease of ~20% up to $\sim 200^\circ\text{C}$ where it leveled off, refer to Figure 2.2. The shape of the curve indicated that any water on the

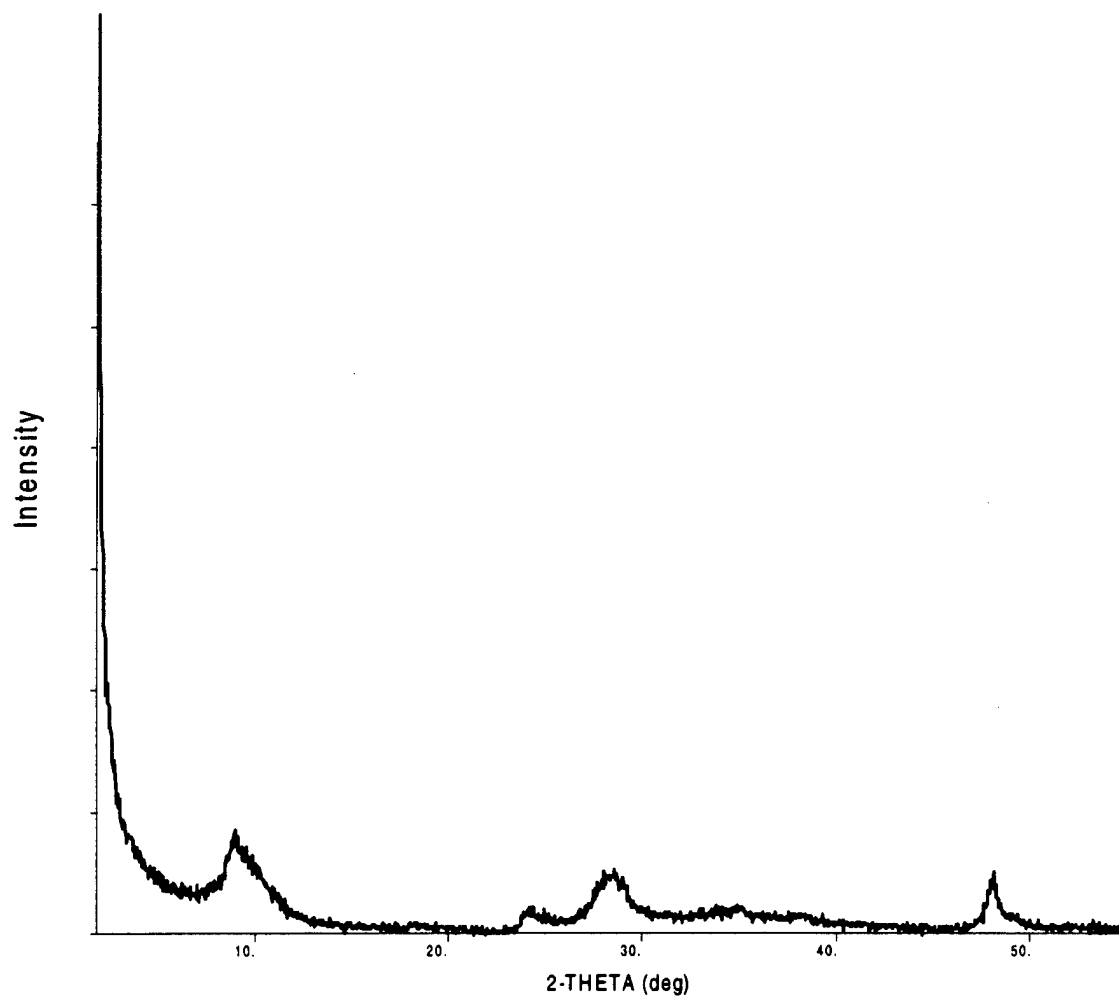


Figure 2.1. XRD pattern of GMG-I-1, the Na titanate sample synthesized with the original parameters.

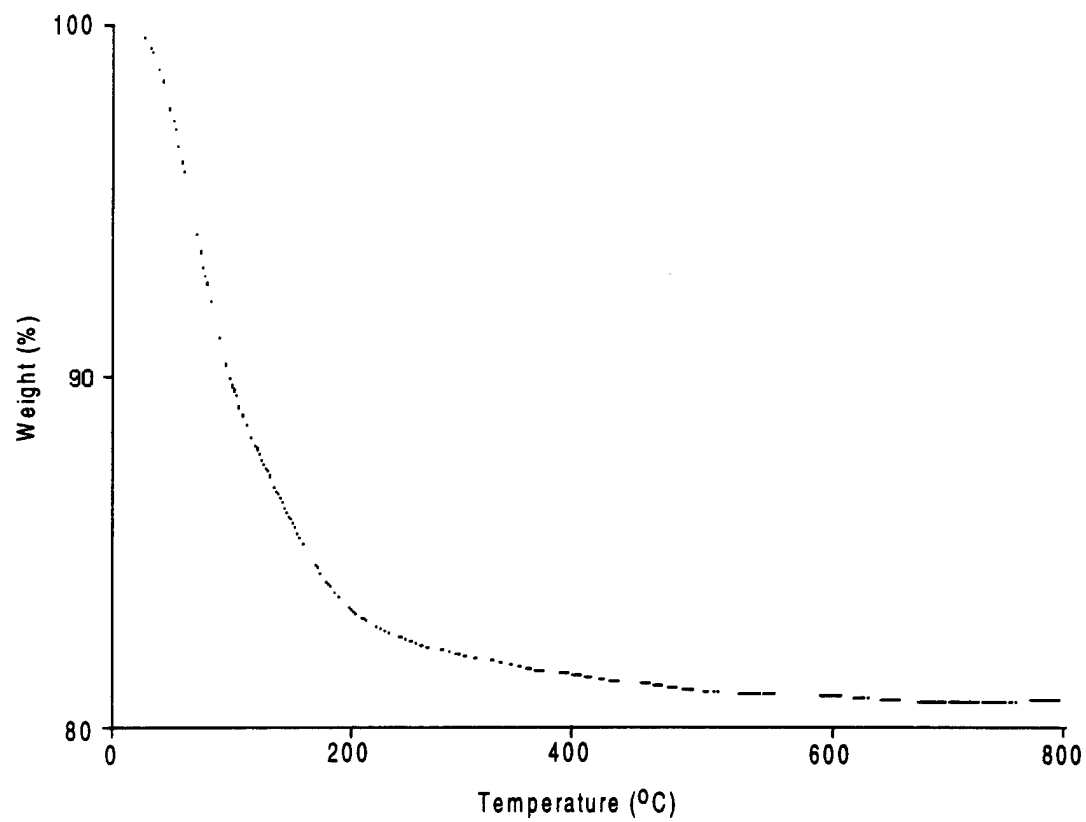


Figure 2.2. Thermogravimetric analysis (TGA) of GMG-I-1.

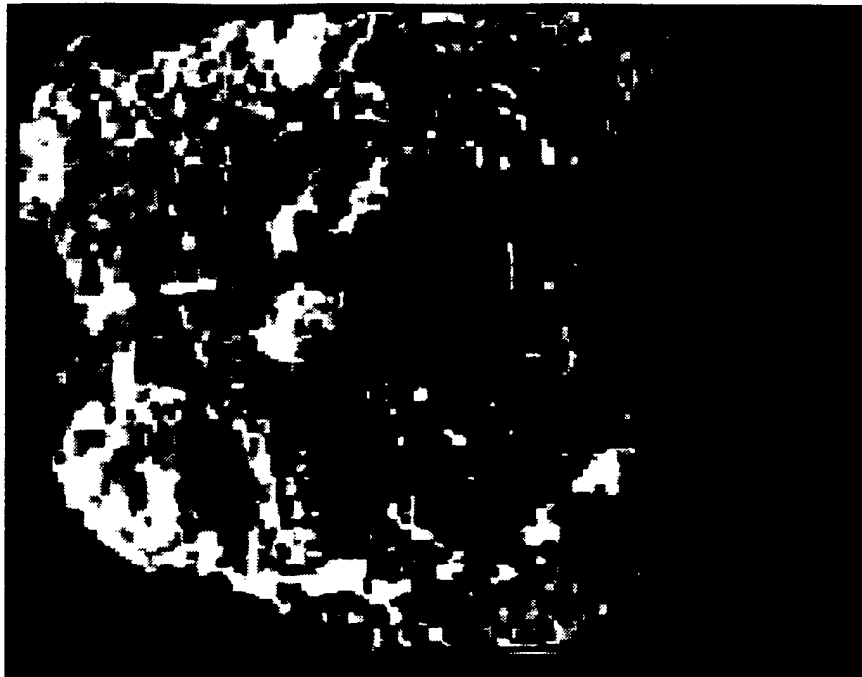


Figure 2.3. Scanning electron micrograph of GMG-I-1 at a magnification of 5000x.

material surface as well as within the framework came off together before 200°C. A scanning electron micrograph was also taken of this original product on a JSM T330A SEM at a magnification of 5000x, indicating that the material was a woolly textured, amorphous aggregate, see Figure 2.3.

Synthesis Variations

A series of syntheses were performed, see Table 2.1, where one parameter within each group, either the heating time, the oven temperature, the Na:Ti mole ratio, or the synthesis heating method, was varied from the original synthesis (GMG-I-1) in order to isolate how each parameter's changes altered the Sr²⁺ uptake of the titanate. For example, in the first series, the original hydrothermal heating time was changed from 1 day to 2, 3, 7, and 30 days while the other parameters were kept constant in each experiment. The hydrothermal oven temperatures were changed from 200°C to 150 and 170°C in the next series, while the Na:Ti mole ratio was altered from 3.90 in the original synthesis to 0.44, 2.00, and 6.00 in another experimental set. Finally, the original heating method included mixing and heating the reactants together for 4 hours in a preheating stage, transferring them into a hydrothermal bomb for pressure heating, and then quickly cooling the bomb under the tap in a fast quenching step. In the last series, one synthesis was conducted where just the preheating stage was omitted from the heating method, in another, the hydrothermal bomb step was left out. In the last, the fast quenching step was changed to slow quenching where the bomb remained inside the oven while the temperature was slowly decreased to room temperature overnight. Once

each of these series was assessed for their effects on the titanate's exchange ability, the variations which improved Sr^{2+} ionic selectivity were pooled together into one optimal titanate synthesis.

Table 2.1 Summary of changes in the titanate synthesis method.

	(days)	(oC)		
	Oven time	Oven temp.	Na:Ti mole ratio	Heating method
GMG-I-1	1	200	3.90	preheating, bomb, fast quench
GMG-I-10a	2	200	3.90	preheating, bomb, fast quench
GMG-I-10b	3	200	3.90	preheating, bomb, fast quench
GMG-I-10c	7	200	3.90	preheating, bomb, fast quench
GMG-I-10d	30	200	3.90	preheating, bomb, fast quench
GMG-I-22a	1	150	3.90	preheating, bomb, fast quench
GMG-I-22b	1	170	3.90	preheating, bomb, fast quench
GMG-I-24a	1	200	0.44	preheating, bomb, fast quench
GMG-I-24b	1	200	2.00	preheating, bomb, fast quench
GMG-I-24c	1	200	6.00	preheating, bomb, fast quench
GMG-I-27	1	200	3.90	<i>bomb, fast quench</i>
GMG-I-28	n/a	n/a	3.90	<i>preheating</i>
GMG-I-39	1	200	3.90	<i>preheating, bomb, over-night quench</i>
GMG-I-59	2	175	6.00	preheating, bomb, fast quench

Hydrothermal Heating Time Variations. In the series GMG-I-10a-d, the heating time was changed from 1 day to 2, 3, 7, and 30 days, respectively. The X-ray patterns of these samples showed peaks which appeared at the same positions as in GMG-I-1, see Figure 2.4. However, as the heating times increased, the peaks became

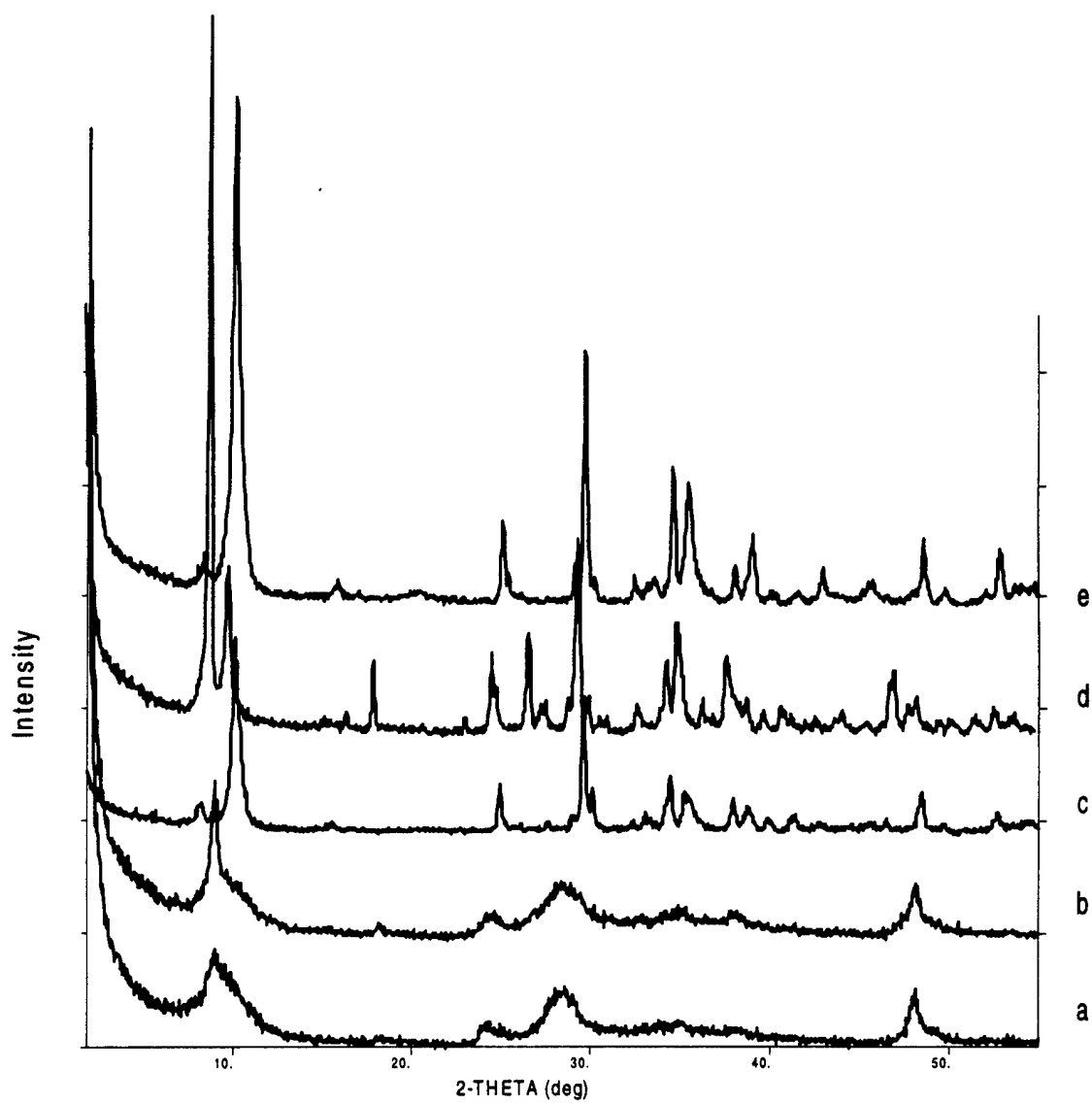


Figure 2.4. XRD pattern of the titanate synthesis with oven time variations. a. GMG-I-1 (1 day), b. GMG-I-10a (2 days), c. GMG-I-10b (3 days), d. GMG-I-10c (7 days), e. GMG-I-10d (30 days).

sharper and more defined. In the original, what was thought to be noise in the 2.3-2.6 Å region developed into peaks at ~2.37, ~2.54, and ~2.6 Å in GMG-I-10b,c,&d. It was also noticed that a splitting of the first peak began to occur in samples GMG-I-10b,c,&d, which, according to Cahill²⁸, may be due to the production of another titanate form. In addition, the XRD pattern for sample GMG-I-10c showed a slight shifting of the peaks, which may be due to a change in the water content between the layers, as well as some additional peaks, which may result from the presence of an impurity.

These data show that the material's structure became more crystalline the longer it was heated in the oven. Because the month long synthesis didn't show much more improvement in crystallinity over the week long synthesis, experiments using longer heating times were not pursued. It appears that one month of heating is necessary for this material to reach its maximum crystallinity which was still not crystalline enough to be able to solve the crystal structure.

A comparison of the TGA patterns of this series revealed that after a heating time of 3 days or more, the material began to develop a second weight loss at 600°C. For example, refer to the TGA of sample GMG-I-10d in Figure 2.5. This indicated that the material became more crystalline and the structure became more rigid to a point where a higher temperature was needed to remove water buried within the framework.

Select materials were run on the SEM, one of which was GMG-I-10d, see Figure 2.6. At a magnification of 1000x, the material appeared to be needle-like crystals, showing further evidence that the longer heating time produced a material which was much more structured than the original GMG-I-1.

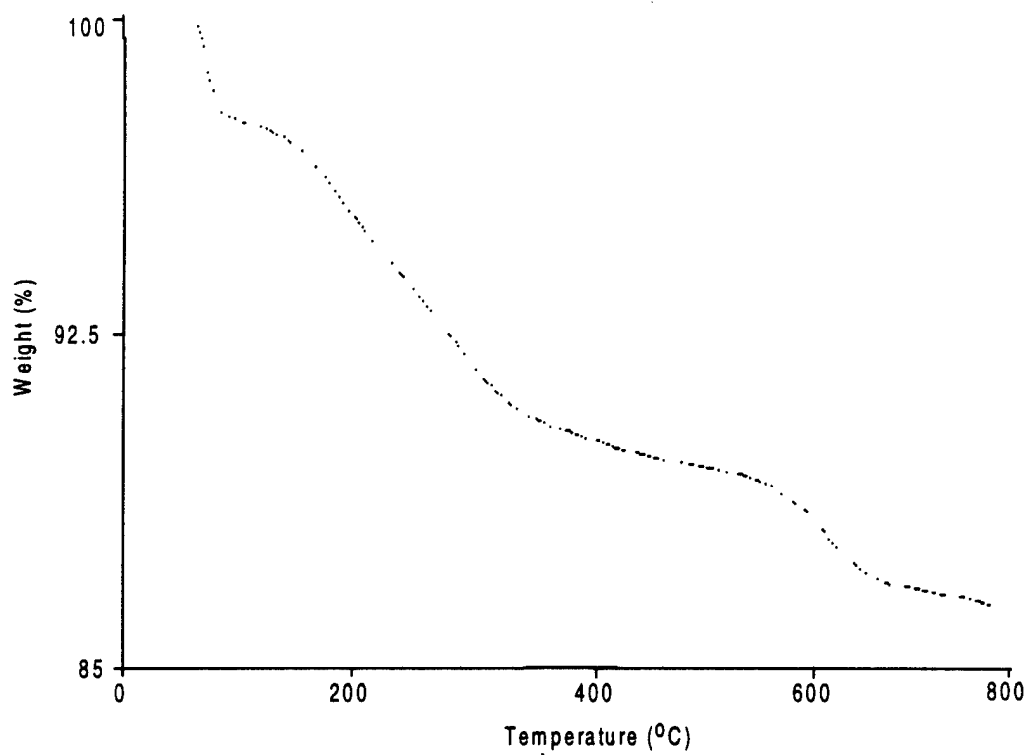


Figure 2.5. Thermogravimetric analysis (TGA) of GMG-I-10d.



Figure 2.6. Scanning electron micrograph of GMG-I-10d at a magnification of 1000x.

Hydrothermal Oven Temperature Variations. In the oven temperature series, the temperature of the oven was varied in GMG-I-22a,b from 200°C to 150 and 170°C, respectively. The X-ray pattern of GMG-I-22b (170°C), see Figure 2.7, was considerably less crystalline than the original 200°C sample, indicating that a decrease in oven temperature, decreases the sample crystallinity, which is in accord with the previous data series. However, as the temperature was further decreased to 150°C in GMG-I-22a, the crystallinity of the product increased. In this case it appears that TiO₂ was present in the sample in the form of Anatase at 2.37 Å and possibly Brookite at 2.97 Å and in the 2.4-2.5 Å range, indicating that a temperature of 150°C was not high enough to completely form the desired Na nonatitanate but partially converted the alkoxide to TiO₂. The TGA patterns were similar to each other, showing a weight loss of ~10% at 200°C, corresponding to surface moisture, and another loss of 20% at 600°C due to loss of internal water.

Na:Ti Mole Ratio Variations. The mole ratio of Na:Ti was varied from 3.9 originally to 0.44, 2.0, and 6.0 in the samples GMG-I-24a,b,c. Again, the X-ray patterns were very broad and as poorly crystalline as GMG-I-1. Changing the amount of base used in the synthesis had no effect on the crystallinity of the titanate, which is in disagreement with the work performed by Cahill²⁸. The TGA patterns of GMG-I-24a&b were similar to the original with one weight loss at 200°C; although, GMG-I-24c displayed two losses of weight at 200 and 600°C.

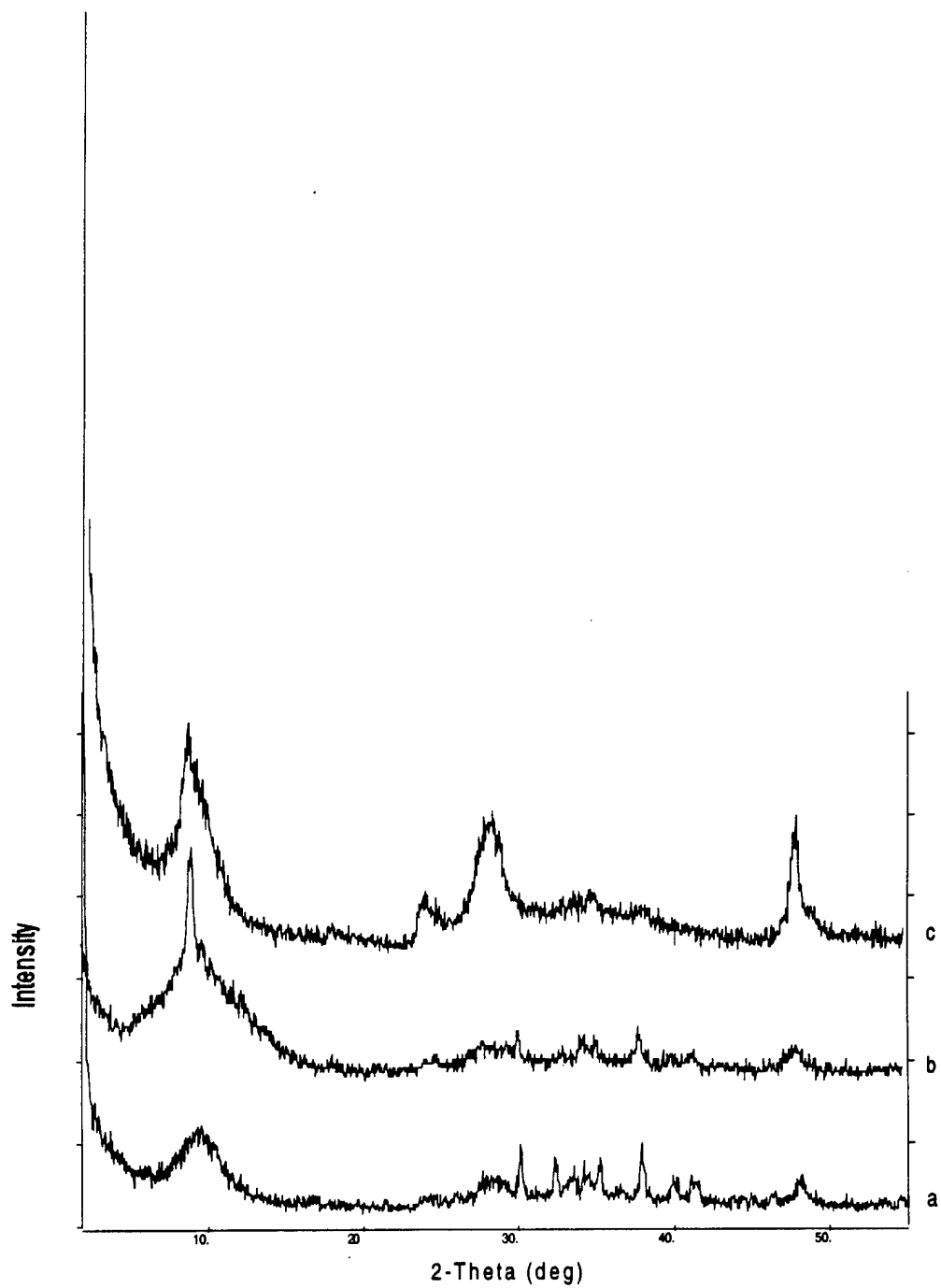


Figure 2.7. XRD pattern of the titanate synthesis with oven temperature variations. a. GMG-I-22a (150°C, scale x10), b. GMG-22b (170°C), c. GMG-I-1 (200°C, scale x10).

Heating Method Variations. The synthesis heating method was altered from the original by omitting just the preheating step in GMG-I-27, by omitting the hydrothermal bomb step in GMG-I-28, and by changing the bomb cooling step from a fast quench under the tap, to a slow quenching step where the bomb temperature was gradually reduced to room temperature overnight in sample GMG-I-39. The X-ray pattern of GMG-I-27 was even more undefined than GMG-I-1 and GMG-I-28 barely had any peaks at all, see Figure 2.8. This indicates that omission of the preheating and hydrothermal steps, respectively, further reduced the crystallinity of the titanate. The X-ray pattern of GMG-I-39 showed that it was of equal crystallinity with GMG-I-1. The TGA patterns of GMG-I-27 and GMG-I-39 indicated two weight losses at 200 and 600°C. However, GMG-I-28 showed one slow slope to ~600°C where it leveled off, indicating its reduced crystallinity due to the omission of the hydrothermal step.

Once the Sr²⁺ ion exchange selectivity was assessed for each of the synthesis variations, see Chapter III, sample GMG-I-59 was produced using all the parameters which maximized the exchange ability. These included using a preheating step on a 6.0 mole ratio mixture of Na:Ti followed by a hydrothermal bomb stage using an oven temperature of 175°C for 2 days and cooling the bomb in a fast quenching step. The X-ray pattern of sample GMG-I-59 was similar to that of the original synthesis; however, its TGA pattern showed 2 weight losses at ~200°C and ~600°C which indicated that this sample may be slightly more crystalline than the first sample due to the longer heating time.

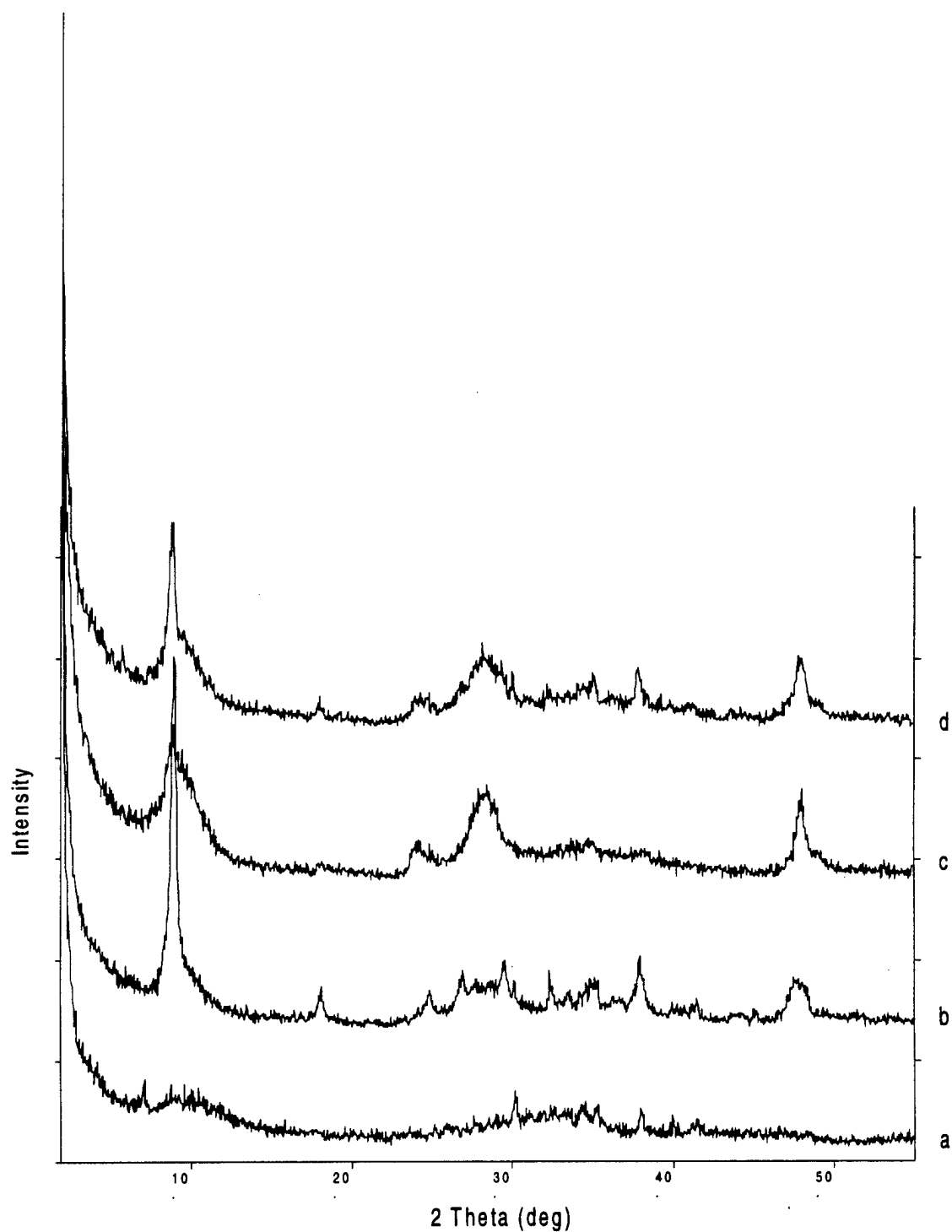


Figure 2.8. XRD pattern of the titanate synthesis with heating method variations. a. GMG-I-28 (w/o bomb), b. GMG-I-27 (w/o preheating), c. GMG-I-1 (original), d. GMG-I-39 (slow quenching).

Of the selected samples used for SEM work, none had a very different appearance from the original material except for GMG-I-10d which showed a drastic change in morphology, as described earlier.

Variations in the Synthesis Reactants

Additional syntheses were attempted in which other reactants were substituted into the original synthesis, refer to Table 2.2. In one experiment, Ti was replaced with the larger Zr metal to determine whether a structure would be formed where larger ion exchange sites may be created. In other syntheses, NaOH was replaced with KOH and CsOH with the idea that again, since these metals are larger than the Na, they would push open the exchange sites making it easier for a large ion such as Sr^{2+} to fit within and also, as with the CsOH sample, create a site specific for Cs^+ ions.

Along similar lines, $\text{Sr}(\text{NO}_3)_2$ was added to the synthesis mixture in addition to NaOH, as $\text{Sr}(\text{OH})_2$ is partially insoluble. This was an attempt to create a titanate structure which formed a perfect fit for the Sr^{2+} ions within the sites and “remembered” or retained that shape after they were washed out with Na, enabling radioactive Sr^{2+} ions to exchange back into a site specific for its size.

In the past, research was conducted where, on the basis of Na titanates such as $\text{Na}_2\text{Ti}_3\text{O}_7$, new compounds, such as KTiNbO_5 , were designed where the Ti^{4+} and Nb^{5+} metal ions were averaged together to act as one metal ion within the structure.²⁹ Upon further investigation of these titanoniobates in their Cs, Rb, and Tl forms, it was found that they may be possible ion exchangers with Cs^+ as the most stable form.³⁰ In

continuation of these ideas, similar research was conducted where Nb was doped into a titanate structure; it was reported that the Nb atoms replaced some of the Ti atoms and were incorporated into the structure, changing it slightly.³¹ The researchers found that this new material showed an increase in Cs⁺ selectivity over the original titanate in waste solutions of 5.7 M Na⁺, especially at pH's greater than 12. With all of this past research in mind, an effort was made to dope Nb into the sodium nonatitanate structure in order to produce a material with improved ion exchange selectivity for Cs⁺ and Sr²⁺.

Table 2.2 Summary of changes in the reactants used for titanate syntheses.

	Reactants used
GMG-I-31	NaOH and Zr isopropoxide
GMG-I-33,34	NaOH, Ti isopropoxide, Sr nitrate
GMG-I-38	GMG-I-1 and Sr nitrate
GMG-I-43	CsOH and Ti isopropoxide
GMG-I-55	KOH and Ti isopropoxide
GMG-I-57	NaOH, Ti isopropoxide, Nb(V) oxide

Replacement of Ti By Zr. In GMG-I-31, 8.4g of a 50% solution of NaOH was added to 12.63g of Zr isopropoxide, Aldrich 70%, which was equimolar to the original Ti(OPr)₄, and the same procedure as described for GMG-I-1 was followed. The purpose of this experiment was to try to produce Na₄Zr₉O₂₀ which, due to the larger Zr metal, may produce larger cation sites making it easier for Sr²⁺ ions to exchange. However, the

product's X-ray pattern showed that ZrO_2 had been formed. This is not an efficient ion exchanger and is therefore of no value in this research. As it was apparent that a "zirconate" exchanger could not be synthesized, no further attempts at this product were made.

Addition of $Sr(NO_3)_2$ to NaOH. Attempts were made to replace NaOH in the synthesis with a Sr material in order to create a customized fit for the Sr^{2+} ions which would be retained after Na^+ was washed back in due to the ion memory effect. Because $Sr(OH)_2$ is partially soluble, $Sr(NO_3)_2$ had to be used in addition to the NaOH base when attempting to make $Sr_2Ti_9O_{20}$. In GMG-I-33, 8.4g of a 50% solution of NaOH was added to 7.7g of $Ti(OPr)_4$ and mixed and heated as usual. The mixture was then transferred to a bomb and instead of adding deionized water, 15 ml of 1M $Sr(NO_3)_2$ in deionized water was added and the procedure continued as normal. The X-ray pattern of the produced material matched that of $SrTiO_3$, which was not what was desired. The material was then divided into two, where one half was washed with 200 ml of 1M HNO_3 , filtered, dried, and X-rayed, then mixed with 200 ml of 1M NaCl, filtered, dried and X-rayed. The other half was mixed and heated with 200 ml of 1M Na_4EDTA at $50^\circ C$ for 1 hour, then filtered, dried, and X-rayed. Each of the following XRD patterns was also of $SrTiO_3$ which meant that Sr^{2+} could not be washed out of the structure and a stable product had been formed.

By using an exact 2 mole Sr : 9 mole Ti ratio (6 ml of 1M $Sr(NO_3)_2$: 7.7 g $Ti(OPr)_4$) and following the previous synthesis method with an oven temperature of

150°C, another attempt was made to force the production of $\text{Sr}_2\text{Ti}_9\text{O}_{20}$ in sample GMG-I-34. The X-ray pattern of the initial product, see Figure 2.9, showed peaks representing $\text{Na}_4\text{Ti}_9\text{O}_{20}$ as well as SrTiO_3 , which indicates that since Sr was a limiting reagent and Na was in excess, SrTiO_3 must have been formed first and the remaining Ti was used to produce $\text{Na}_4\text{Ti}_9\text{O}_{20}$. This also leads to the conclusion that in any mixture of Sr and Ti, production of SrTiO_3 is favored over $\text{Sr}_2\text{Ti}_9\text{O}_{20}$. At that point, the experiment was stopped as it was obvious that an exchangeable Sr titanate could not readily be produced by direct synthetic methods.

As it was noted that SrTiO_3 is a favored and stable product, its production was attempted where Sr^{2+} was mixed and heated with a previously formed Na nonatitanate which would provide an option for producing a stable, safe product after active Sr is exchanged into the titanates. In GMG-I-38a,b, 0.96 ml of 1M $\text{Sr}(\text{NO}_3)_2$ were loaded into each 1g sample of GMG-I-1 at 50% capacity using enough deionized water to provide a moist mixture. The samples were shaken for 3 hours, filtered, and washed with deionized water. Mixture "a" was transferred to a bomb with a few ml's of water and mixture "b" was put into a Zr crucible before they were both heated in an oven at 150°C for 1 day. After mixture "a" was quenched, filtered, and dried, XRD patterns were taken of both samples. The patterns were the same as the original titanate with some contaminations; indicating that the Sr had not reacted to form SrTiO_3 . Mixture "b" was replaced into the crucible and heated for 1 day at 300°C giving an X-ray pattern which still showed no change. The material was then heated again at 500°C for 1 day. Here the pattern started to show the development of two small SrTiO_3 peaks at 2.78 and 1.96

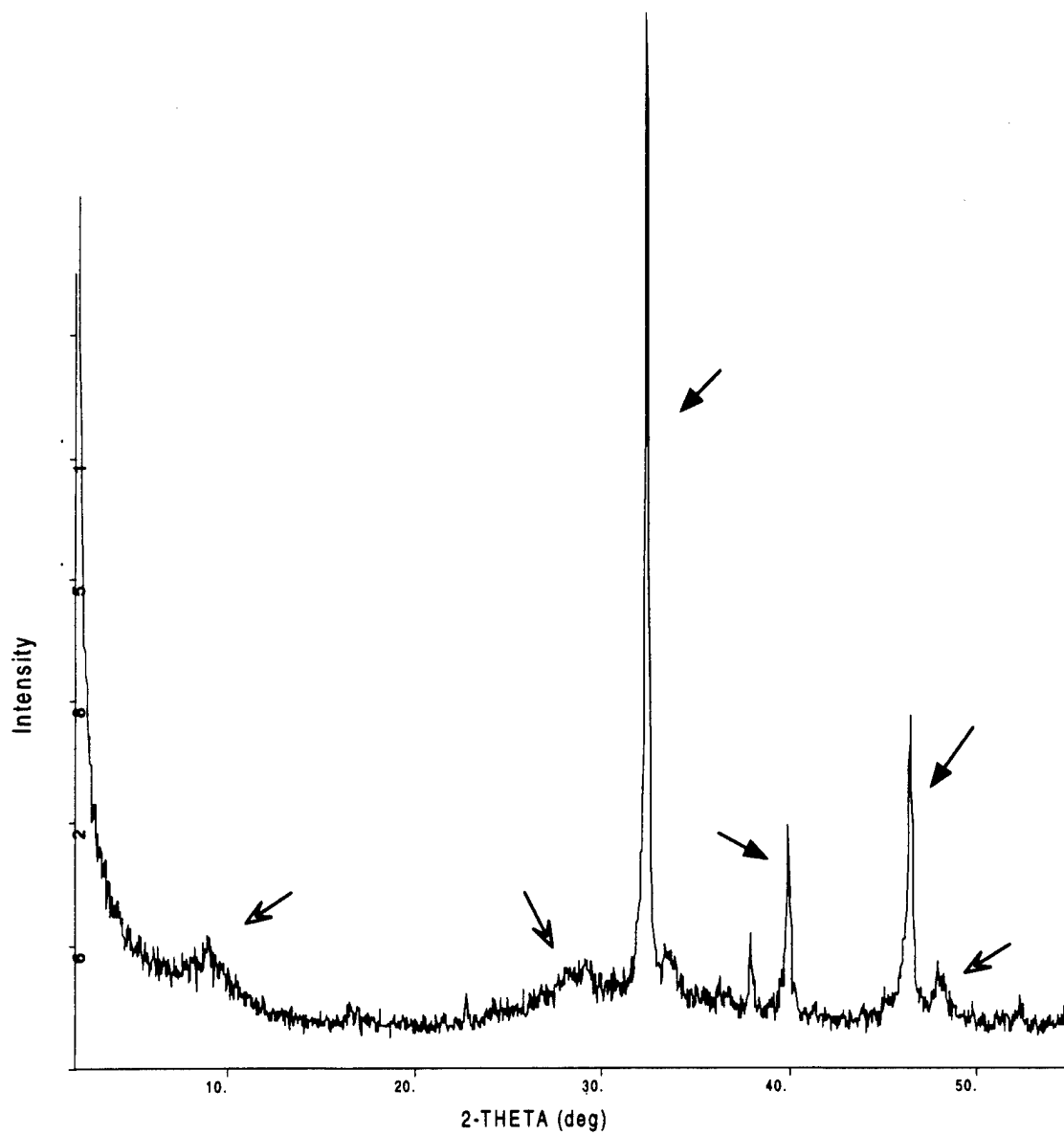


Figure 2.9. XRD pattern of GMG-I-34, Sr titanate synthesis where SrTiO₃ (closed arrows) formed with Na₄Ti₉O₂₀ (open arrows).

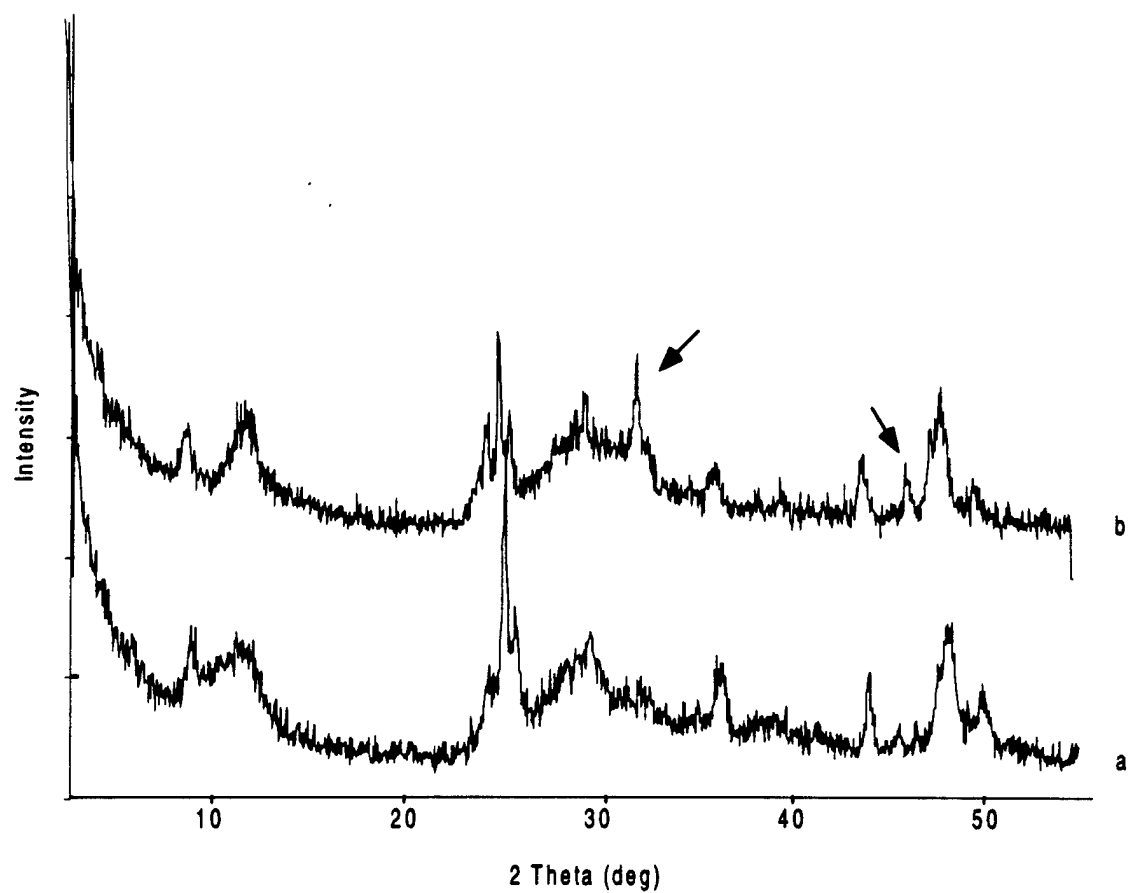


Figure 2.10. XRD pattern of the SrTiO₃ synthesis, a. GMG-I-38b1 (300°C), b. GMG-I-38b2 (500°C). The arrows indicate where SrTiO₃ peaks began to emerge.

Å, see Figure 2.10. In conclusion, after active Sr is exchanged into the titanate, the mixture needs to be heated to a temperature of at least 500°C in order to form the stable SrTiO₃ product.

Replacement of NaOH with CsOH and KOH. An experiment was run in GMG-I-43 where Cs₄Ti₉O₂₀ production was attempted in order to allow the Cs⁺ ions to create larger ion exchange sites which, would be perfectly fitted for Cs⁺ exchange according to the previously mentioned ion memory effect and may make it easier for the large Sr²⁺ ions to exchange within. Here, NaOH was replaced with an equimolar amount of a 50% solution of CsOH (44.97g) using the same method of preparation as in GMG-I-1. The first XRD pattern showed a broad peak at 6.9 Å and a small one at 3.19 Å, see Figure 2.11. This slightly resembled a typical titanate pattern, giving evidence that a Cs titanate was formed. The TGA pattern was typical as well with a weight loss of 10% at ~200°C and another loss of 3% at 600°C. The product was then washed with acid, NaCl, and Na₄EDTA in the same manner as in GMG-I-33. After the Cs⁺ was flushed out and the Na⁺ was washed back in, the X-ray pattern, as seen in Figure 2.11, began to more closely resemble the original titanate with typical peaks at 3.5, 2.3, and 1.89 Å. This indicates that the Na-form may have reformed.

This same procedure was utilized in GMG-I-55 where an equimolar amount of a 50% solution of KOH (11.8g) replaced NaOH in an effort to form K₄Ti₉O₂₀ where, similarly, the K⁺ ions may enlarge the exchange sites. However, the X-ray pattern in Figure 2.12 showed the material to be a possible mixture of K₂Ti₆O₁₃ (peaks 7.76 and

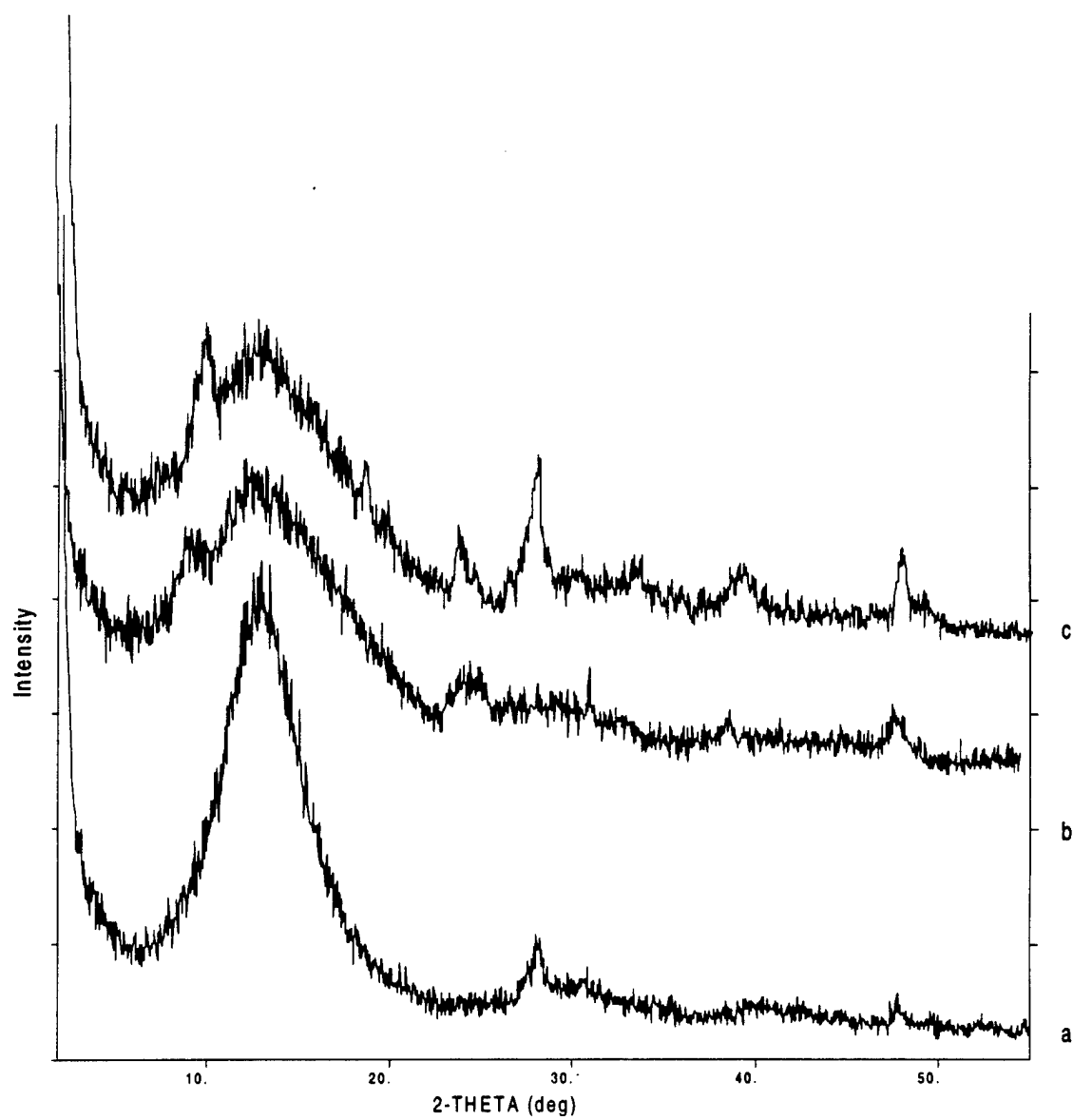


Figure 2.11. XRD pattern of the Cs titanate synthesis. a. GMG-I-43 (Cs titanate before washing), b. GMG-I-43a1 (after NaCl wash), c. GMG-I-43b (after Na₄EDTA wash).

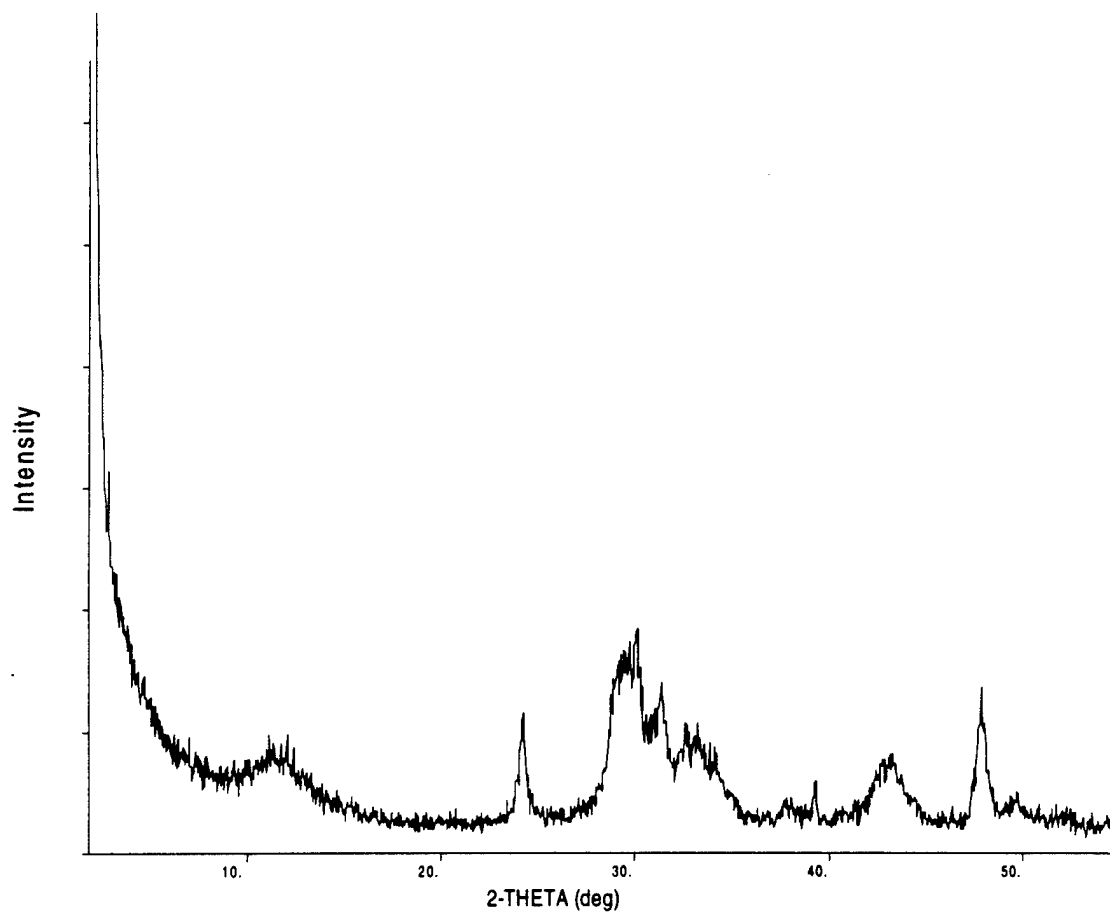


Figure 2.12. XRD pattern of GMG-I-55, the K titanate synthesis, which shows a mixture of $K_2Ti_6O_{13}$ and $K_2Ti_8O_{17}$.

2.97 Å) and $K_2Ti_8O_{17}$ (peaks 7.76, 3.67, and 3.0 Å), according to the JCPDS Powder Diffraction File from the International Centre for Diffraction Data. The TGA pattern resembled some of the other titanates with weight losses at 200°C and 600°C. The X-ray patterns taken of the samples after the K^+ ions were washed out with Na^+ , using the same method as in sample GMG-I-43, were shown to be identical to the original product but far less crystalline, indicating that the K^+ ions were unable to be exchanged.

Nb Doping. A process was examined in GMG-I-57 where Nb was doped into the titanate structure for 10% of the Ti atoms in order to try to improve the exchange efficiency, according to previous data.^{29,30,31} 9.0g of a 50% solution of NaOH was added to a mixture of 6.9g of $Ti(OPr)_4$ and 0.718g of Nb_2O_5 using the GMG-I-10a synthesis method, where it was heated in the oven for two days to ensure complete reaction. After the filter/washing step, no precipitate was noticed in the filtrate so it can be said that Nb was in the sample but not necessarily within the structure. The XRD, again, followed the same pattern as the original GMG-I-1 except for one out of place peak at 4.78 Å which does not represent free Nb_2O_5 so therefore may be due to Nb within the titanate structure, see Figure 2.13. The TGA pattern showed a 17% weight loss at 200°C, then leveled off to 600°C where the material lost an additional ~4% in weight. However, not even elemental analysis testing can confirm whether or not Nb was incorporated into the structure so the next step is to look for improvements in the material's ion exchange selectivity.

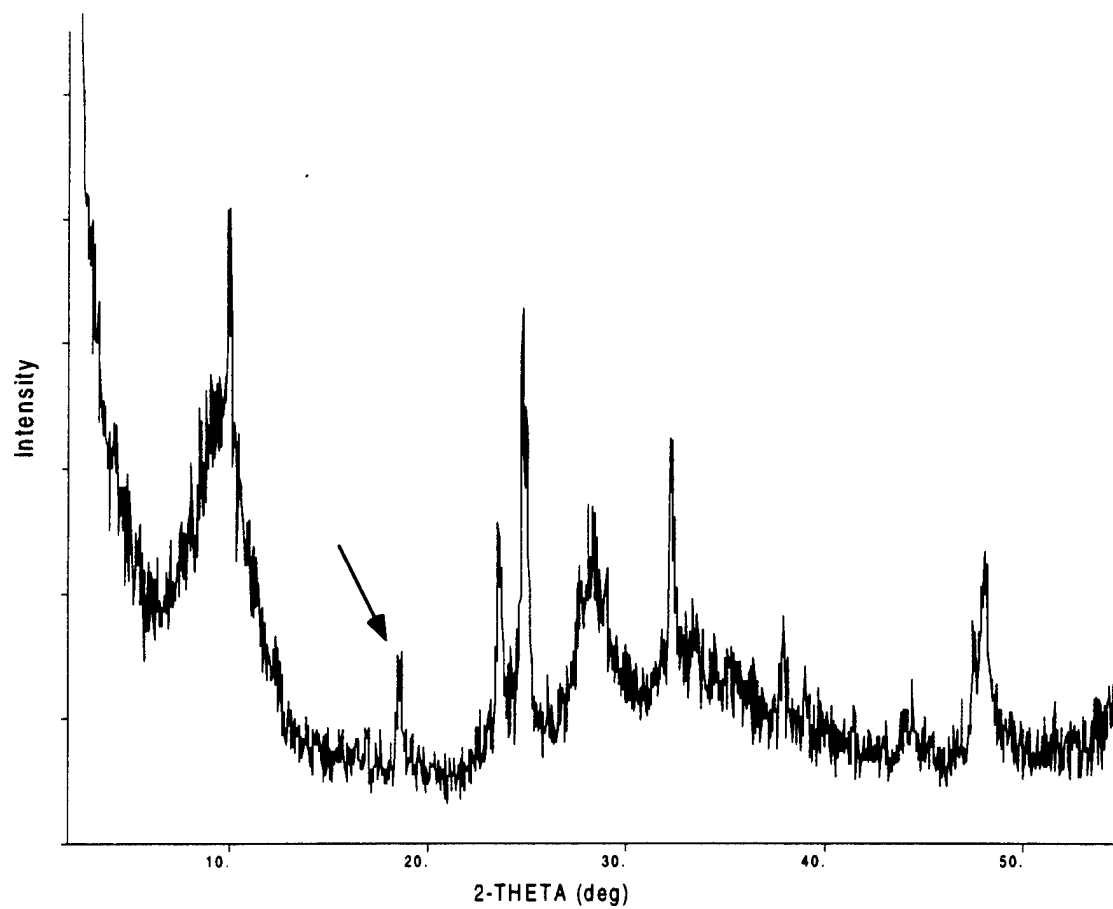


Figure 2.13. XRD pattern of GMG-I-57, the Nb doped sample. The arrow points to a possible Nb peak.

CHAPTER III

ION EXCHANGE PROPERTIES

K_d Determinations

The distribution coefficient (K_d) measures the selectivity of a material for a specific ion by fixing the ion concentration in the initial solution and determining the concentration in the solution after it's been contacted with the material. The difference indicates the amount of ion that was exchanged into the compound and allows the K_d to be calculated according to the following equation:

$$K_d = (C_i - C_f) / C_f \times (V/m) \quad (3.1)$$

where C_i is the initial solution concentration, C_f is the final concentration, V is the volume of the solution (ml), and m is the mass of the exchanger (g).

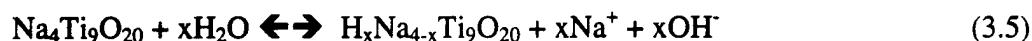
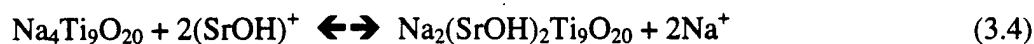
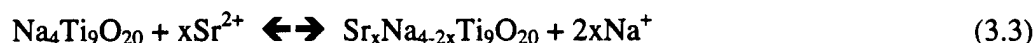
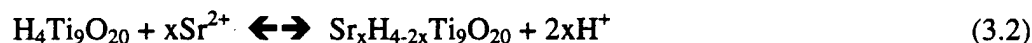
Assessment of GMG-I-1. Batch tests were performed on GMG-I-1 with alkaline earth metals to measure the selectivity of the titanate for each metal in the group.

Approximately 0.1g of GMG-I-1 was added to 10 ml of solution containing 0.001M $M(\text{NO}_3)_2$, where $M = \text{Mg, Ca, Sr, or Ba}$ each with increasing concentrations of NaNO_3 at 0.001, 0.01, 0.1, 1.0 M in order to see how the uptake of each metal was affected by Na^+ . (This would provide a better idea of how the material would perform in actual waste as Na is one of the main tank waste components.) These mixtures were gently shaken for 24 hours using a rotary shaker, then filtered through #42 Whatman filter paper; the pH's of the final equilibrated solutions were ~11. The filtrates and initial solutions were analyzed for Mg, Ca and Ba using a Varian A250 Atomic Absorption

Spectrophotometer. Sr solutions, each of which contained an additional ^{89}Sr spike of 0.4 mg of total Sr/l, were analyzed by a radiotracer technique. One ml of the Sr filtrates and initial solutions were mixed with 5 ml of scintillation cocktail and analyzed using a WALLAC 1410 Liquid Scintillation Counter to determine the ^{89}Sr activity.

The K_d values showed that the titanate was most selective for Sr^{2+} over the range of Na concentrations, see Figure 3.1. The values for Mg^{2+} , Ca^{2+} , and Ba^{2+} were all much lower than the Sr^{2+} K_d values indicating that these ions are less suited for exchange into the titanate exchange sites than Sr^{2+} ions.

The K_d 's for Mg, Ca, and Ba showed a slight decrease as the Na^+ ion concentration increased. The Sr K_d 's initially increased with increasing Na^+ ion concentration, then dropped off as the Na^+ solutions became more concentrated. These observations can be explained according to the following equations adapted from Lehto, et al.²⁶



At very low Na^+ concentrations, the Na titanate is partially hydrolyzed to the H-form, raising the solution pH and impeding Sr^{2+} exchange as the titanate prefers to be in its H-form. However, once the solution has reached equilibrium, and Na^+ ions are added, as seen in eq 3.5, the solution equilibrium is driven to the left to produce more Na titanate which can more effectively exchange Sr^{2+} . Therefore, as the concentration of Na^+ in the

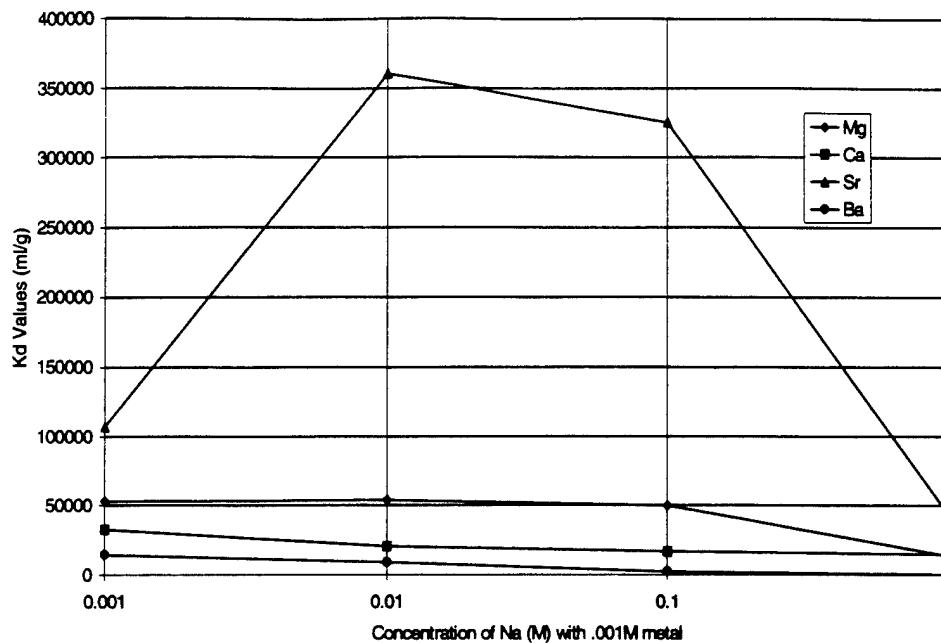


Figure 3.1. K_d graph assessing the ion exchange selectivity of GMG-I-1 for alkaline earth metals.

exchange solution increases, the exchange efficiency improves until a point where the concentration is too high, causing the excess Na^+ ions to compete with the alkaline earth metals for exchange sites which reduces the material's exchange efficiency. This maximum concentration is reached at 0.01M Na^+ in Sr solutions and at 0.001M Na^+ in Mg, Ca, and Ba solutions (although the variation in K_d 's over the range of Na^+ concentrations was minor.)

Once the selectivity for the alkaline metals was assessed, K_d batch tests were run on each series of syntheses, which are described in the previous chapter, and the effects

of increasing concentrations of each of the competing Na, Mg, Ca, and Ba ions on ^{89}Sr exchange were determined using the previously described procedure.

Hydrothermal Heating Time Variations. In the first series, GMG-I-10a-d, where the oven heating times were increased from 1 day to 2, 3, 7 and 30 days, respectively, the K_d values increased from the original 1 day heated sample to the 2 day heated sample but decreased in the samples heated any longer, refer to Figure 3.2. It was noted that the crystallinity of the original sample was poor and did not improve in the next sample; however, the crystallinity began to drastically improve as the sample was heated for 3 days and longer, (see Figure 2.4). Therefore, the more crystalline and rigid the material became, the less efficient it was for Sr^{2+} removal.

Overall, for each set of data using the different competing ions, Sr K_d results were greatest in the presence of Na^+ ions, decreased approximately equally with Mg^{2+} and Ba^{2+} , and offered the lowest results for Ca^{2+} solutions. Since the titanate prefers to exchange with divalent cations, Na^+ is the least competitive with Sr^{2+} for ionic uptake. Along with the fact that some Na^+ can enhance ion exchange, by causing a shift in equilibrium as seen in eqs 3.2-3.5, Na^+ provides the best Sr^{2+} ion exchange data. Mg^{2+} and Ba^{2+} are more competitive with Sr^{2+} than Na^+ due to their valency; however, because Mg^{2+} , (ionic radius of 0.65 Å), is too small and Ba^{2+} , (ionic radius of 1.35 Å), is too large compared to Sr^{2+} , (ionic radius of 1.13 Å), their competition for exchange sites is reduced which explains their average K_d values. Ca^{2+} , (ionic radius of 0.99 Å), on the other hand, is close to the size of Sr^{2+} which makes it very competitive for the

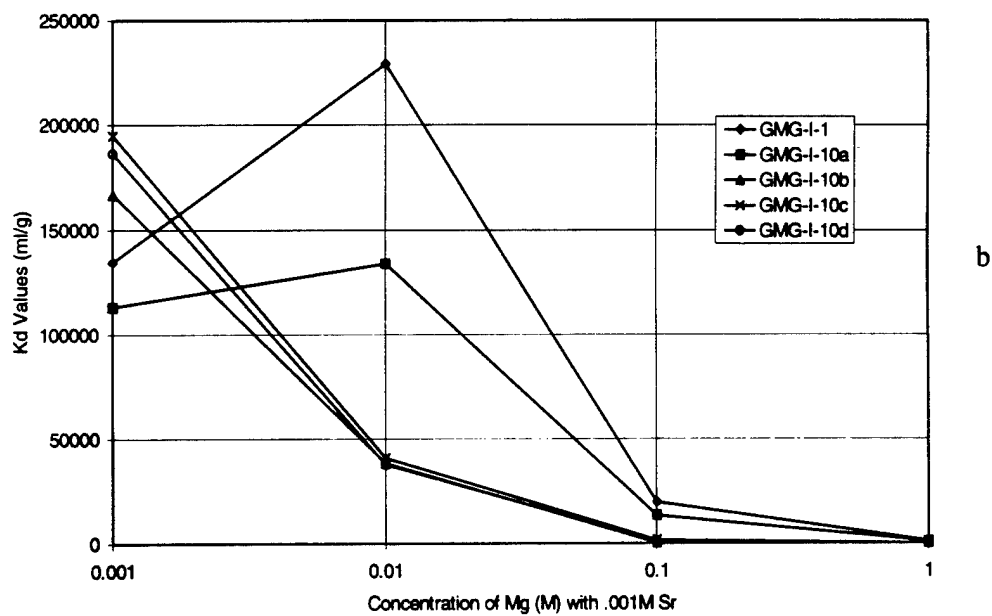
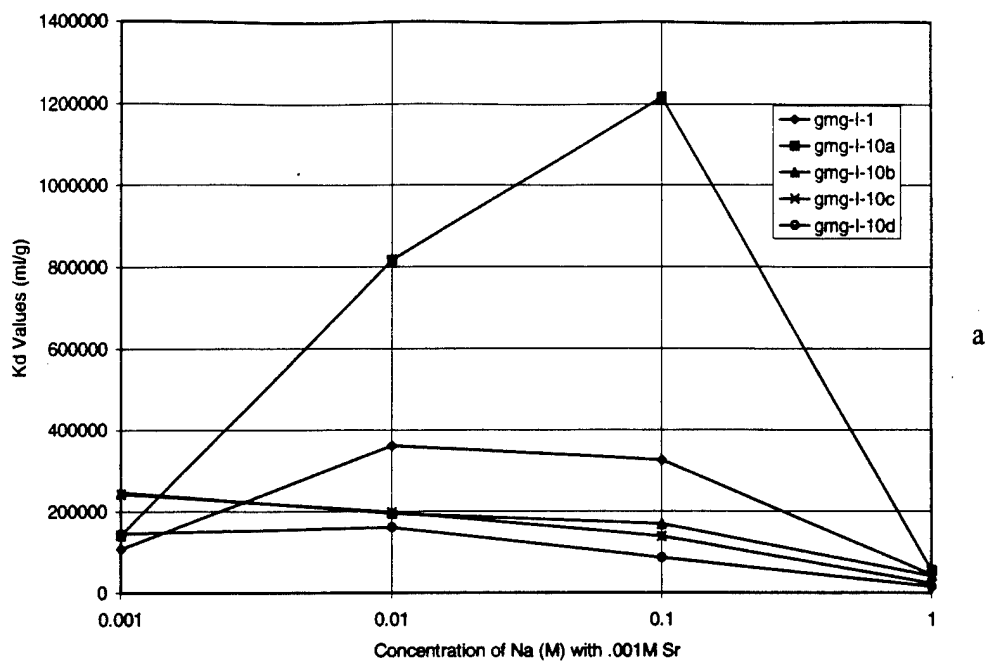


Figure 3.2. K_d graphs of the heating time variation series, samples GMG-I-1 & 10a-d, in a. Na/Sr, b. Mg/Sr, c. Ca/Sr, and d. Ba/Sr solutions.

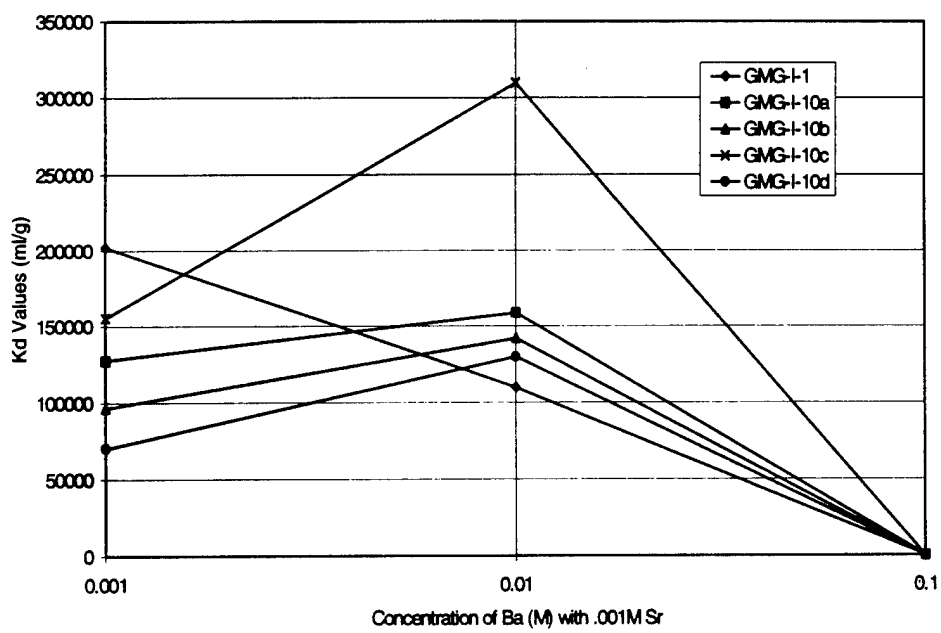
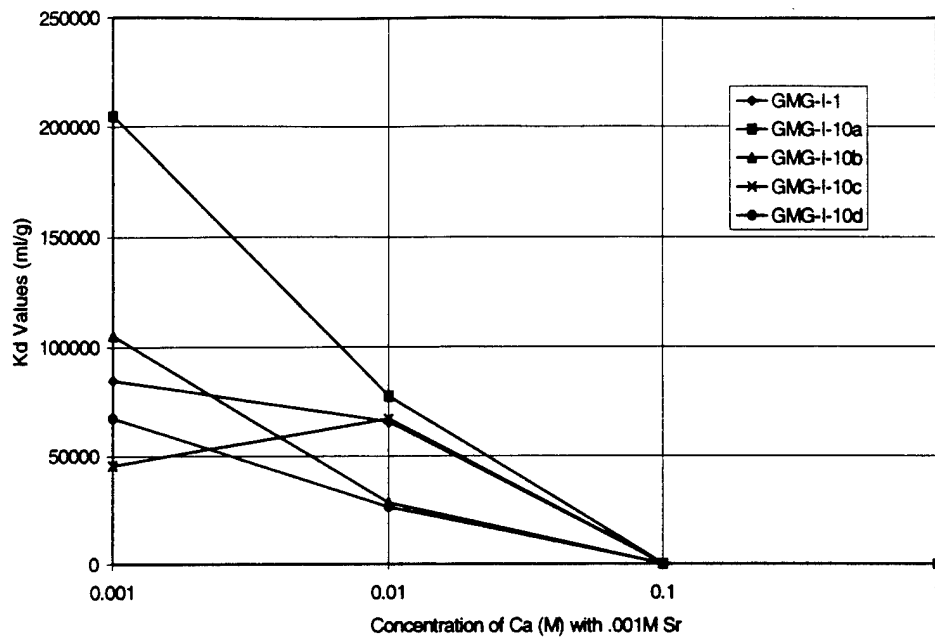
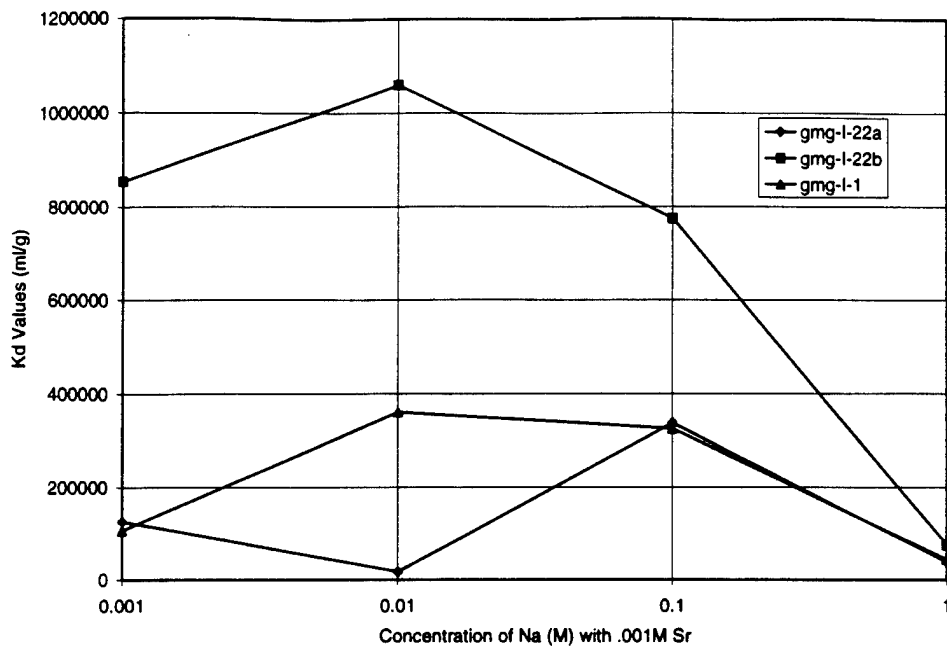


Figure 3.2. Continued.

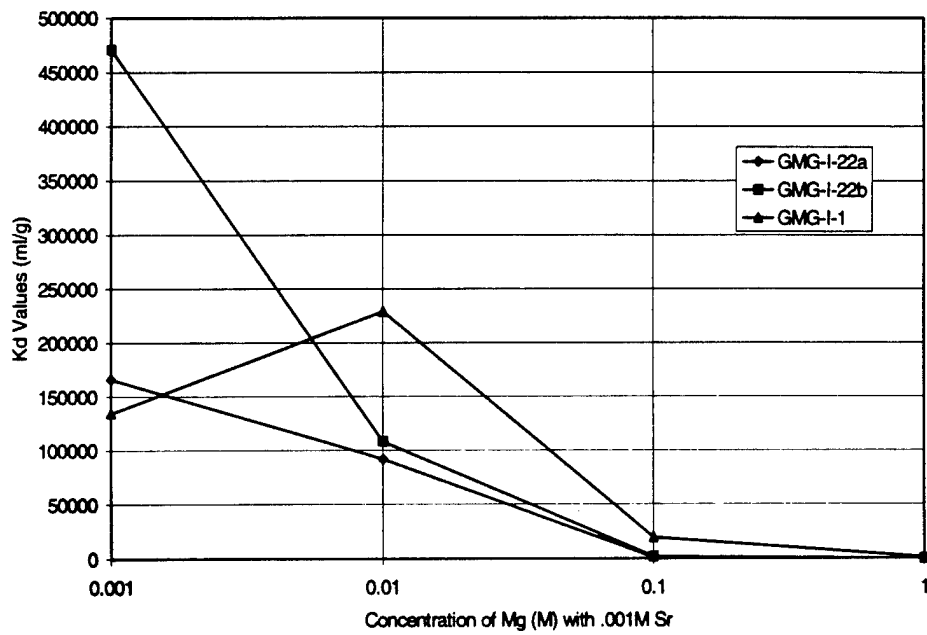
exchange sites on the titanate. Therefore, as the Ca^{2+} ions vie for and block open sites, the Sr^{2+} K_d 's are the lowest in Ca^{2+} solutions.

The K_d values for samples GMG-I-1 & 10a in both Na and Mg/Sr solutions as well as GMG-I-10c in Ca/Sr and GMG-I-10a, b, c, & d in Ba/Sr solutions increased with increasing metal ion concentrations, then began to decrease as the concentrations of supporting electrolyte rose too high. Meanwhile the K_d 's of samples GMG-I-10b, c, & d in both Na and Mg/Sr solutions, GMG-I-1, 10a, b, & d in Ca/Sr solutions, and GMG-I-1 in Ba/Sr solutions began to decrease at the lowest metal concentration. As mentioned previously, this is due to the fact that the metal ions may enhance exchange until a point where the metal is too concentrated and begins to block Sr^{2+} exchange sites. This maximum point occurred at different concentrations for each sample in each metal solution due to the fact that each synthesis variation potentially changed the material's exchange sites which would alter its metal selectivities. It was also noted that with Ca/Sr solutions, at 0.1 M Ca and above there is a drastic drop in K_d values, from ~100% Sr^{2+} uptake to ~20%, indicating once again how competitive Ca^{2+} ions are with Sr^{2+} ions for titanate exchange sites.

Hydrothermal Oven Temperature Variations. In the next series of syntheses the oven temperature was changed from the original 200°C to 150°C and 170°C in samples GMG-I-22a and 22b, respectively. Overall, the K_d values seemed to be best for the 170°C sample, see Figure 3.3. According to the previous data, it would be expected that the best ion exchange results would come from the least crystalline sample which



a



b

Figure 3.3. K_d graphs of the temperature variation series, samples GMG-I-1, 22a, & 22b in a. Na/Sr, b. Mg/Sr, c. Ca/Sr, and d. Ba/Sr solutions.

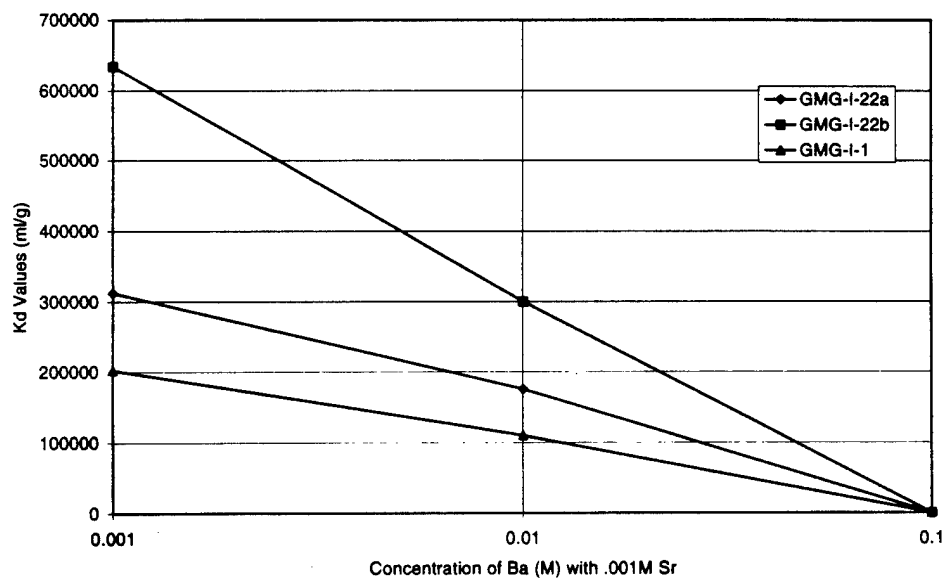
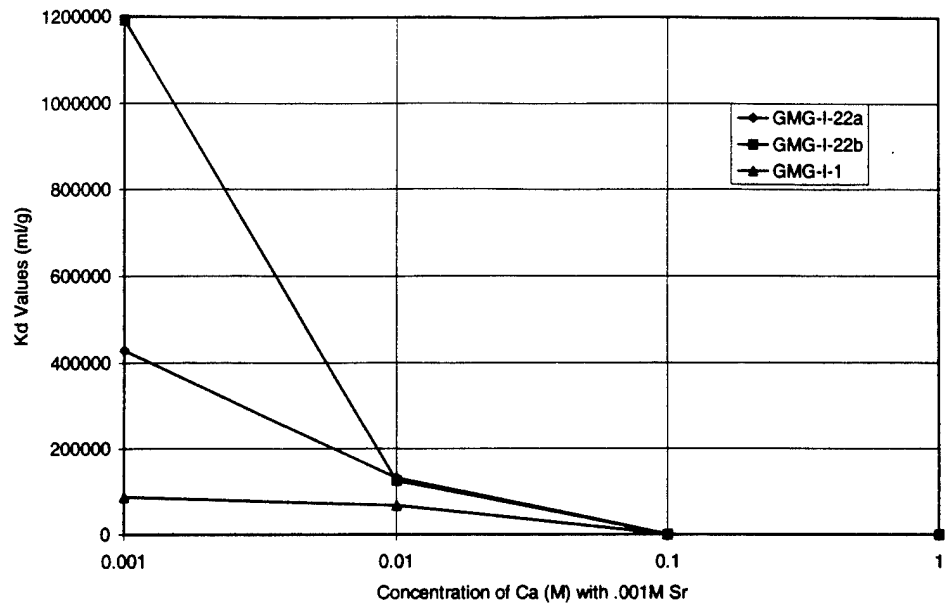


Figure 3.3. Continued.

was expected to be GMG-I-22a. However, from XRD patterns it was found that this sample was mostly TiO_2 , as a temperature of 150°C was not high enough to form the Na nonatitanate. Subsequently, sample GMG-I-22b (170°C) was found to be the least crystalline titanate in this series, which correlates this set of K_d values to the previous data.

As for each set of Metal/Sr exchange data in this series, the tests using Na^+ ions gave the best results because they provide less competition for Sr^{2+} than the other metals due to the titanate's affinity for divalent ions. Sr K_d tests using the Ba^{2+} solutions also produced high K_d 's due to the fact that Ba^{2+} is too large for the titanate exchange sites to pose much of a hindrance to the competing Sr^{2+} ions, which is in accordance with the previous data. The Mg^{2+} and Ca^{2+} batch test results offered the lowest Sr^{2+} uptake values because their sizes are closer to Sr^{2+} than the other metals, providing more competition for Sr^{2+} in the exchange process. This is slightly different from the data offered in the heating time variation series which indicated Mg^{2+} was too small for the titanate sites produced in GMG-I-10a-d.

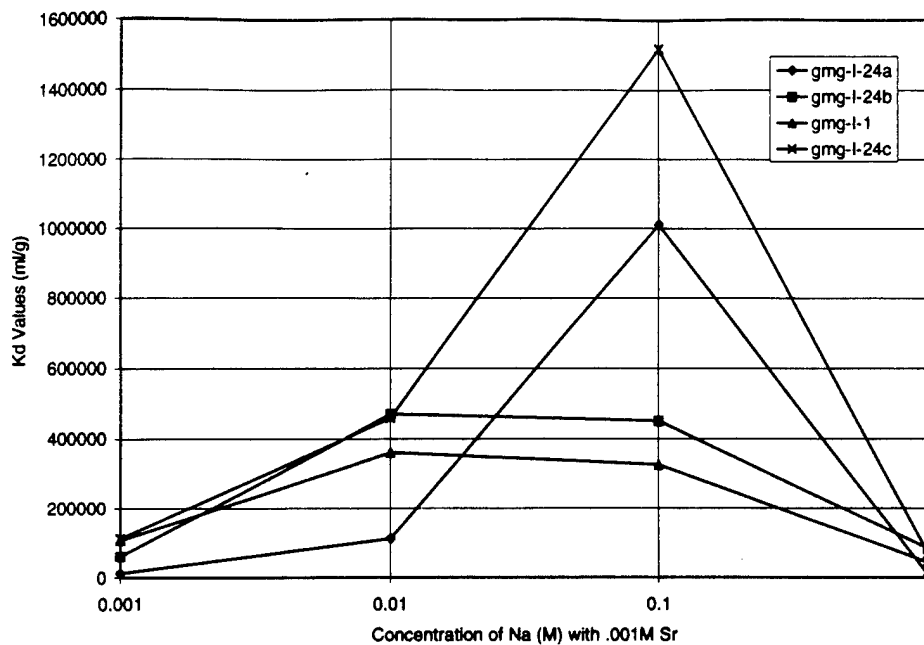
Within each set of Metal/Sr K_d data, the basic trends which were observed in the heating time variation series were also found here. The Sr^{2+} uptake for samples GMG-I-1, 22a, & 22b was enhanced with increasing Na^+ concentration until a point where Na^+ ions begin to compete for exchange sites and lower the K_d values. Also, Sr^{2+} uptake for GMG-I-1, 22a & 22b was initially hindered by increasing concentrations of the competing Mg, Ca, and Ba ions, such that at concentrations of 0.1M and greater, the ions began to reach the capacity of the titanate's exchange sites and drastically reduce Sr^{2+}

uptake to nearly zero. This indicates that the titanates produced in this temperature variation series have a lower selectivity for Sr^{2+} over other group II metals.

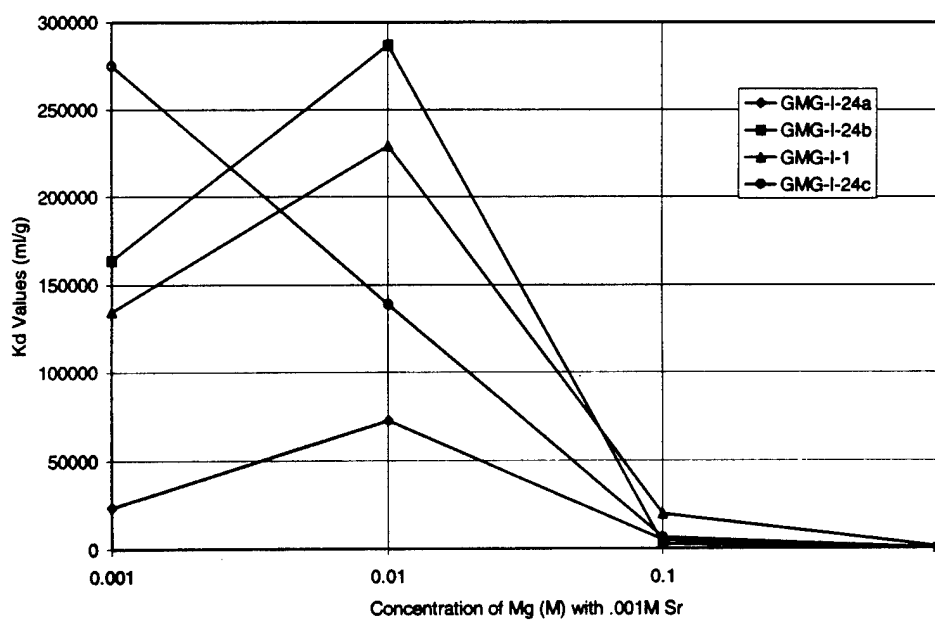
Na:Ti Mole Ratio Variations. In the next series where the Na:Ti mole ratio was varied in the preparation of samples GMG-I-24a, 24b, & 24c, the crystallinity of the products was not affected, so predictions of the materials' ability for Sr^{2+} uptake could not be made simply by looking at their XRD patterns. However, in solutions of Na/Sr, it was apparent that the sample with the largest Na:Ti mole ratio, GMG-I-24c, gave the best Sr K_d results. For the most part, as the materials' Na:Ti mole ratios decreased, their respective Sr K_d results in Na solutions decreased as well. In the Group II Metal/Sr solutions, this trend wasn't as obvious; although, it seemed that in general the best results came from sample GMG-I-24c, see Figure 3.4.

As with the heating time and temperature variation series, the best Sr^{2+} K_d 's for this series came from the Na/Sr solutions as the titanate isn't as inclined to exchange univalent ions. Again, the large Ba^{2+} radius inhibits its exchange into the titanate sites allowing for more efficient Sr^{2+} exchange. As Mg^{2+} and Ca^{2+} are closer in size to Sr^{2+} , they provide the most competition for Sr^{2+} uptake, resulting in the lowest K_d values.

This series also displayed the same general trends for each individual batch test where K_d values for samples GMG-I-24c in Mg/Sr solutions and GMG-I-1 & 24c in Ca and Ba/Sr solutions decreased with increasing metal concentration, and K_d values for samples GMG-I-1, 24a, b, & c in Na/Sr solutions, GMG-I-1, 24a & b in Mg/Sr solutions, and GMG-I-24a & b in Ca and Ba/Sr solutions initially increased then decreased

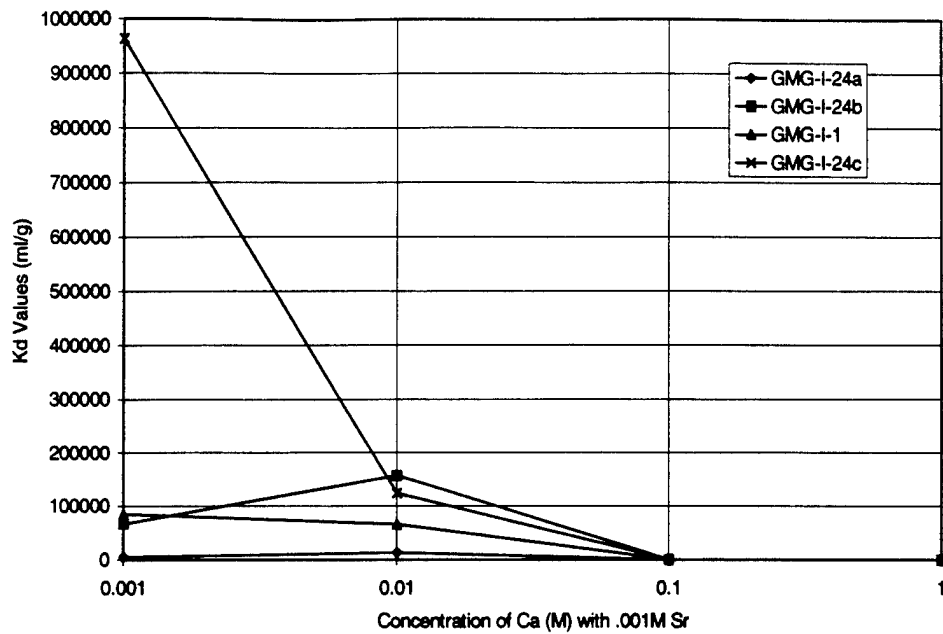


a

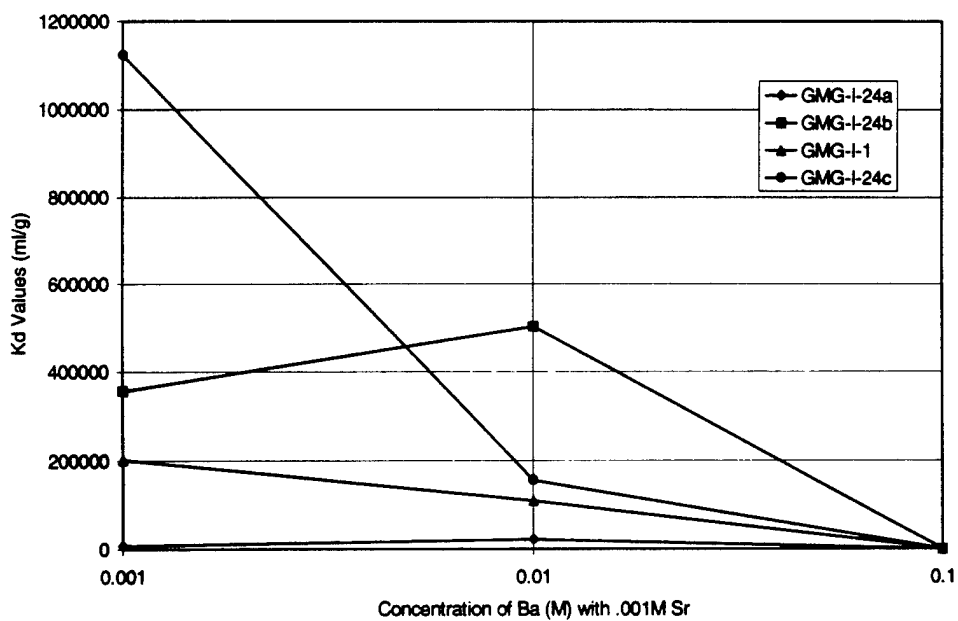


b

Figure 3.4. K_d graphs of the Na:Ti mole ratio variation series, samples GMG-I-1, 24a, 24b, & 24c in a. Na/Sr, b. Mg/Sr, c. Ca/Sr, and d. Ba/Sr solutions.



c



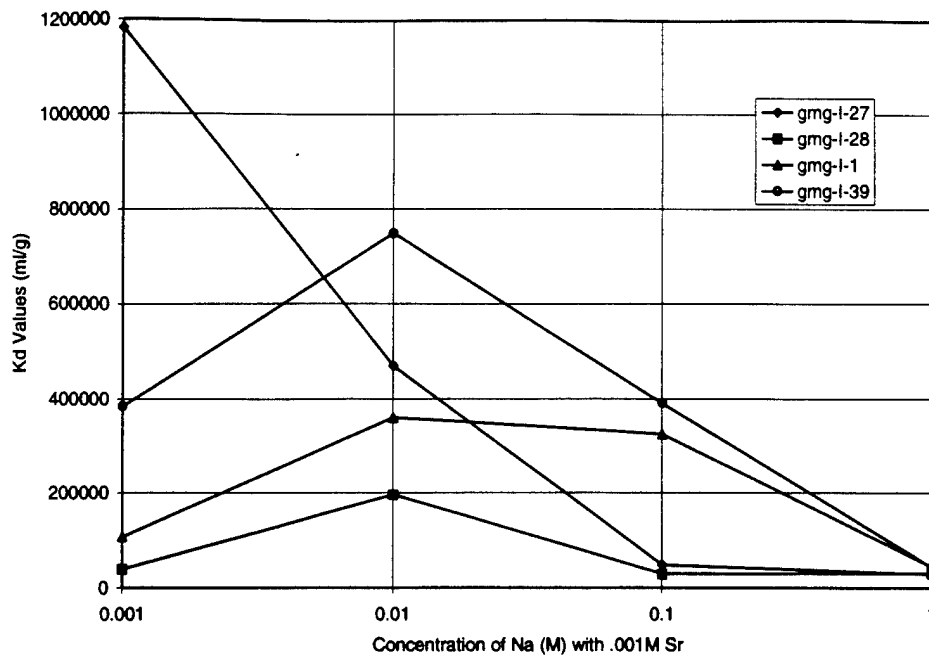
d

Figure 3.4. Continued.

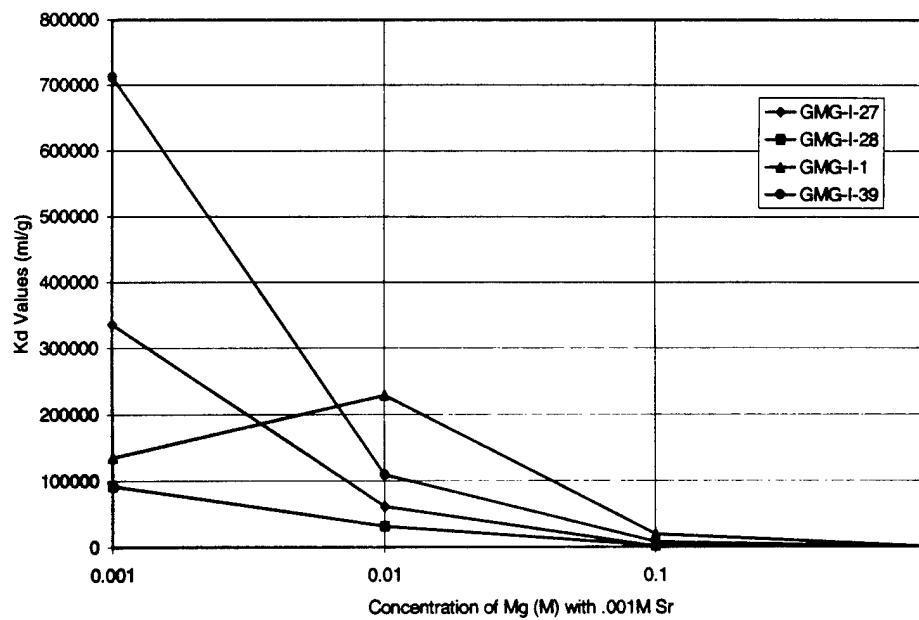
depending on the concentration at which the metal ions began to compete with Sr^{2+} for uptake into the titanate exchange sites.

Heating Method Variations. In the final synthesis variation series, the heating method was altered where the 3 hour preheating step was omitted in GMG-I-27, the bomb step was omitted in GMG-I-28, and the bomb quenching step was changed from quick cooling under tap water to slow cooling in the oven overnight in GMG-I-39. The XRD pattern of GMG-I-28 was the most amorphous in this series as would be expected due to the omission of the hydrothermal step. However, since this mixture was only heated to 100°C , the product was probably not Na nonatitanate, but a hydrous titanium dioxide, as was evidenced in sample GMG-I-22a which was heated at 150°C . Sample GMG-I-27 was less crystalline than sample GMG-I-39 which was of equal crystallinity to the original sample, GMG-I-1. It would be expected that GMG-I-27 would have the best Sr selectivity according to previous data; however, GMG-I-39 generally gave the highest K_d 's, refer to Figure 3.5. GMG-I-27 may not have been structured enough to be able to have a high Sr selectivity, but GMG-I-39, which had been in the oven almost as long as GMG-I-10a, (the 2 day sample), due to its cool down time, had become an ideal structure for optimal Sr^{2+} exchange.

As seen before, the K_d values of these materials in Na/Sr solutions were slightly higher than the values for the Group II Metal/Sr solutions; however, the data for the Group II metals were comparable to each other which was not in accordance with previous data. It was also noted that in Mg, Ca, and Ba solutions, at concentrations of



a



b

Figure 3.5. K_d graphs of the heating method variation series, samples GMG-I-1, 27, 28 & 39 in a. Na/Sr, b. Mg/Sr, c. Ca/Sr, and d. Ba/Sr solutions.

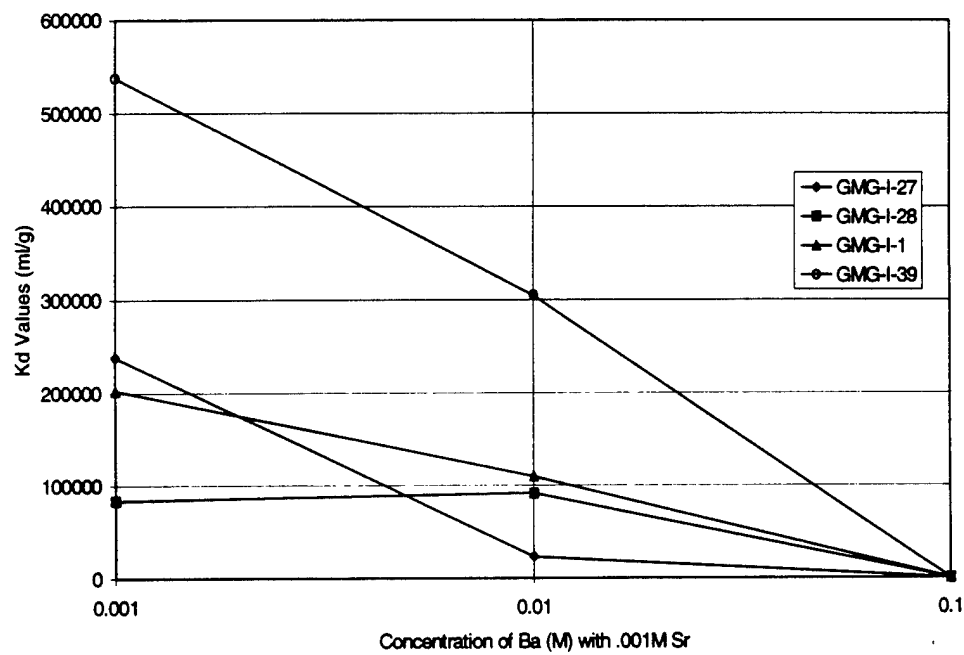
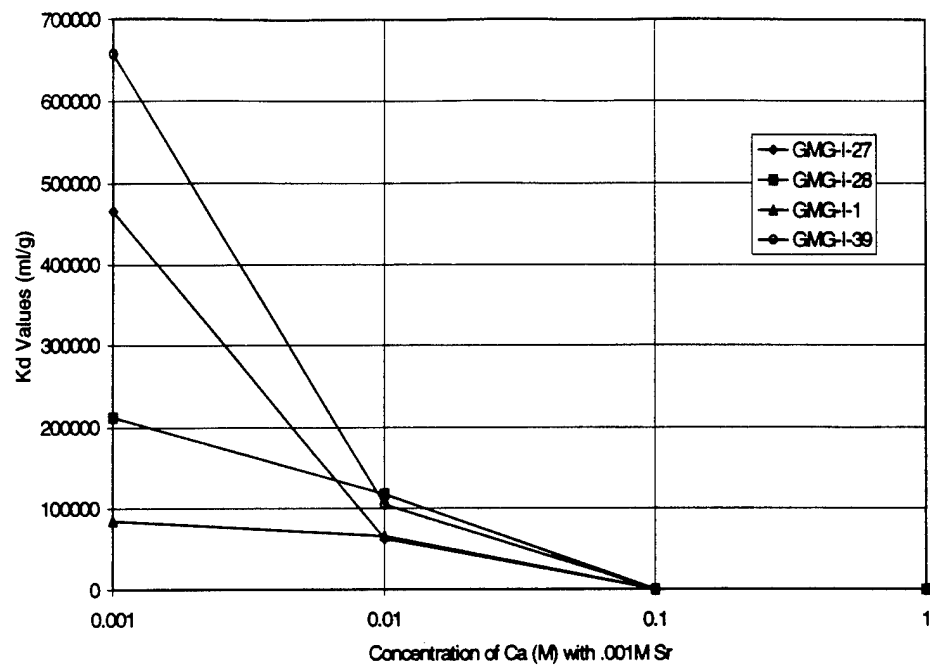


Figure 3.5. Continued.

0.1 M and greater, these ions began to provide a great hindrance to Sr exchange for the samples in this heating method variation series by reaching the ion exchange capacity of the material which drastically reduced the Sr K_d values to zero.

After the performance of each series was measured, a synthesis was conducted (sample GMG-I-59) where the changes from each series which provided the best Sr²⁺ uptake values were used in order to produce a material that was optimized for Sr exchange. The synthesis used an oven temperature of 170°C for 2 days utilizing the largest Na:Ti mole ratio, 6.00, and the original heating method which included a 3 hour preheating step followed by the hydrothermal bomb step which was quenched quickly under the tap. Although the slow quench variation was the best synthesis sample in its series, if used in addition to a 2 day oven heating time, the sample would be in the oven close to 3 days which is where the K_d results began to decrease in the heating time variation series. The final product showed a vast improvement in Sr²⁺ uptake over the original synthesis, GMG-I-1, in Metal/Sr solutions; however, in Mg/Sr solutions the new sample didn't perform as well, possibly because this material formed exchange sites which were more suited for Mg²⁺ uptake, see Table 3.1.

Variations in the Synthesis Reactants. In addition to the synthesis method variations, compounds were produced where other elements were substituted for Ti and Na. However, the only materials produced that were possible ion exchangers were samples GMG-I-43 where NaOH was substituted by CsOH, GMG-I-55 where NaOH was substituted by KOH, and GMG-I-57 where Nb was doped into the titanate structure.

Table 3.1. Comparison of K_d values for GMG-I-1 and GMG-I-59 in Na/Sr, Mg/Sr, Ca/Sr, and Ba/Sr solutions.

Solutions	(ml/g)	(ml/g)
	GMG-I-1 K_d 's	GMG-I-59 K_d 's
.001M Na/ .001M Sr	107,100	1,344,400
.01M Na/ .001M Sr	360,700	965,100
.1M Na/ .001M Sr	325,000	420,800
1.0M Na/ .001M Sr	43,700	124,700
.001M Mg/ .001M Sr	134,600	106,000
.01M Mg/ .001M Sr	229,200	65,700
.1M Mg/ .001M Sr	19,500	5,000
1.0M Mg/ .001M Sr	1,100	200
.001M Ca/ .001M Sr	84,800	546,900
.01M Ca/ .001M Sr	65,800	126,900
.1M Ca/ .001M Sr	30	50
1.0M Ca/ .001M Sr	10	1
.001M Ba/ .001M Sr	202,200	577,100
.01M Ba/ .001M Sr	109,900	239,800
.1M Ba/ .001M Sr	200	300

Before running any batch tests on the material, sample GMG-I-43 was divided into two, where one half was washed with 1M HNO₃ then 1M NaCl and the other half was washed with 1M Na₄EDTA in order to exchange Cs⁺ for Na⁺. Once the final products were tested for Sr²⁺ uptake in Na/Sr solutions, it became apparent from the poor K_d results of <100 that Na⁺ ions weren't exchanged into the sites or the structures were altered such that the sites could not properly accommodate Sr²⁺ ions. Before sample GMG-I-55 was washed in a manner similar to GMG-I-43, it was tested for Sr²⁺ exchange in Na/Sr solutions where its K_d 's, <142,000, were considerably less than the original sample,

GMG-I-1. The XRD patterns of the washed samples indicated that although K^+ was not removed, much less crystalline products had been formed; as a result of this amorphous structure, the Sr^{2+} exchange selectivity had been drastically reduced to values of <20 . In Na/Sr solutions, the Sr^{2+} K_d results for the Nb doped sample, which was heated in the oven for 2 days, were comparable to the non-doped 2 day sample, GMG-I-10a, which indicates that either Nb was not doped into the structure, or if it was doped in that this process did not improve the structure's ability for Sr^{2+} exchange. Because of the poor results from each of these syntheses, none were pursued any further.

Waste Simulant Batch Tests

NCAW Simulant. These materials were also examined for their exchange selectivity in simulated Hanford tank waste solutions in order to obtain a better idea of how they will perform in actual tank wastes should they be considered candidates for industrial use. 0.05g of each sample from GMG-I-1-10d was added to 10 ml of NCAW solution, (which is a simulation of Tank #241-AZ-102 with over 200 g/L Na^+ and over 150 g/L Al^{3+} , see Table 3.2), along with a ^{89}Sr spike to give a total Sr concentration of 0.4 mg/l, using the same procedure as described in previous batch tests.

Even though sample GMG-I-10a was optimized for Sr^{2+} uptake in Metal/Sr solutions, it was not the most efficient at Sr^{2+} removal in NCAW simulant. The exchange sites produced by this 2 day synthesis were more suited to accommodate Sr^{2+} uptake in the simple Metal/Sr solutions than in the NCAW simulant which included a mixture of competing ions. Therefore, the best results for Sr^{2+} uptake in this waste came

Table 3.2. Compositions of tank waste simulants, NCAW, 101SY-Cs5, and N-Springs, courtesy of G. N. Brown of Pacific Northwest National Laboratory

Species	Concentration (M)		
	NCAW	101SY-Cs5	N-Springs
Al	0.43	0.42	0
Ba	0	0	1.12E-07
Ca	0	4.20E-03	7.27E-07
Cs (inactive)	5.00E-04	4.19E-05	0
Fe	0	1.96E-04	0
K	0.12	0.034	0
Mg	0	0	2.16E-04
Mo	0	4.20E-04	0
Na	4.99	5.1	2.61E-04
Ni	0	2.50E-04	0
Rb	5.00E-05	4.20E-06	0
Sr (inactive)	0	2.90E-07	1.48E-06
Zn	0	5.00E-04	0
carbonate	0.23	0.038	1.25E-04
chloride	0	0	4.51E-05
fluoride	0.09	0.092	1.05E-05
hydroxide	3.4	3.78	n/a
hydroxide (free)	1.68	2.11	1.66E-03
nitrate	1.67	1.29	1.94E-04
nitrite	0.43	1.09	0
sulfate	0.15	4.75E-03	2.16E-04
phosphate	0.025	0.02	0
citric acid	0	5.00E-03	0
tetrasodium EDTA	0	5.00E-03	0
N-(2-hydroxyethyl) EDTA	0	3.75E-03	0
iminodiacetic acid	0	0.031	0
nitriloacetate	0	2.50E-04	0
sodium gluconate	0	0.013	0
Theoretical pH	14.5	14.4	11.2

from the original synthesis, GMG-I-1, with a K_d of 250,100. The K_d values of GMG-I-10b, c & d continued to decrease as the samples' heating times increased as shown in Table 3.3. In comparison to the performance of other materials such as Na titanosilicate, $\text{Na}_2\text{Ti}_2\text{O}_3\text{SiO}_4 \cdot 2\text{H}_2\text{O}$, and K titanosilicate, $\text{HK}_3(\text{TiO})_4(\text{SiO}_4)_3 \cdot 4\text{H}_2\text{O}$, which gave K_d 's of 269,500 and 20,200, respectively, in NCAW waste simulant³², GMG-I-1 seemed to be a rather competitive candidate for industrial use.

Table 3.3. Sr K_d values for samples GMG-I-1-10d in NCAW waste simulant.

	(ml/g)
Sample	Sr K_d Values
GMG-I-1	250,100
GMG-I-10a	143,700
GMG-I-10b	44,700
GMG-I-10c	14,600
GMG-I-10d	600

101SY Simulant. Another batch experiment was conducted on GMG-I-1 in a waste simulation of Tank 101SY which contains numerous complexants such as EDTA, HEDTA, and citric acid which chelate the Sr^{2+} ions making their removal difficult, see Table 3.2. As a result, a very low K_d value (295 at a 200:1 volume to mass ratio) was produced; however, compared to other materials, such as Na titanosilicate and K titanosilicate which gave K_d values of 231 and 31, respectively³², these values were quite high for this type of waste.

Table 3.4. Cs K_d values for all titanate samples in N-Springs waste simulant.

Sample	(ml/g) Cs K_d Values
GMG-I-1	1,160
GMG-I-10a	860
GMG-I-10b	90
GMG-I-10c	120
GMG-I-10d	2
GMG-I-22a	220
GMG-I-22b	320
GMG-I-24a	3,740
GMG-I-24b	510
GMG-I-24c	460
GMG-I-27	310
GMG-I-28	280
GMG-I-39	730
GMG-I-43a1	5,230
GMG-I-43b	250
GMG-I-55	50
GMG-I-57	470
GMG-I-59	190

N-Springs Simulant. Similarly, using the N-Springs waste simulant, (which is a simulation of an alkaline groundwater, see Table 3.2), each of the exchangeable titanates synthesized in this work were looked at for their ^{137}Cs exchange selectivity, following the same procedure used in the previous simulant batch test experiments. Most of the titanates had little affinity for Cs^+ due to its large ionic size (1.69 Å) as was evidenced by the K_d values of <1200, see Table 3.4; however, sample GMG-I-24a which used the exact stoichiometric Na:Ti mole ratio of 4:9, offered a K_d of 3740 which indicated that its structure formed exchange sites which were more favorable for the uptake of Cs^+ ions. Particular interest was given to sample GMG-I-43 which was synthesized with CsOH , in an attempt to create sites perfectly fitted for Cs^+ , before the sample was

washed out with Na^+ in preparation for ion exchange tests. Sample GMG-I-43a which was washed with acid, then NaCl gave a Cs^+ uptake value of only 5230, while GMG-I-43b which was washed with Na_4EDTA gave K_d results of 250, indicating that the EDTA did a poor job of chelating and removing the Cs^+ ions from the sites before the ^{137}Cs exchange tests. In all, these tests show that regardless of how the Na nonatitanate was synthesized, it was a poor Cs^+ exchanger.

pH Batch Tests

A final batch experiment was run on sample GMG-I-1 to investigate the effects of pH on this material's uptake of Sr^{2+} . A solution of 0.001 M Sr / 0.01 M Na with a ^{89}Sr spike (0.4 mg total Sr/l) was divided into 5x25 ml aliquots and by adding either 50% NaOH or concentrated HNO_3 to each, the pH's were made to range from 1.6 to 12.4. The activity of each pH solution was measured on the scintillation counter before 10 ml of each was added to vials containing 0.1g of the titanate which were shaken for 24 hours and filtered as before. Because the Na form of the titanate will exchange Na^+ for H^+ ions when in acidic solution, the pH of the solutions should increase after shaking; therefore, the pH of the filtrate was measured along with its ^{89}Sr activity.

It was expected that the results from this test would correlate with Lehto, et al.²⁶ who showed that low pH will cause a decrease in Sr^{2+} exchange due to the Na titanate undergoing exchange to produce the H-form which, because it is the preferred ionic state, would be slow to exchange with Sr^{2+} . They also showed that an increase in pH would cause an increase in Sr^{2+} uptake due to the OH^- ions forcing an equilibrium shift

to the Na-form which is the more favorable state for ion exchange, refer to eqs 3.2-3.5. However, after shaking the solutions, the pH's ranged from 8.3 to 12.7. Due to this high alkalinity, the titanate was able to remove enough Sr^{2+} ions from solution so that the activities of the filtrates were below the detection limit of the scintillation counter so the expected range of K_d 's could not be observed.

Column Tests

NCAW Simulant. In order to obtain a better idea of how the titanate would perform in an industrial cleanup setting with a constant flow of active effluent through the material, small scale column tests were run on titanate beads which were made by adding enough inorganic binder (about 50%) to 0.1-0.2g of GMG-I-1 to create a moist aggregate. This mixture was stirred until it was homogeneous, then it was spread onto a Teflon plate to sit for 1 hour. After drying in an 80°C oven for 12 hours, the product was ground up slightly and passed through a 40/60 mesh sieve. The beads produced from this process were slurried in 1M NaOH and packed into a 1.5 ml bed volume in a 1.0 x 5.0 cm Kontes Flex Column. Tygon tubing with an inner diameter of 1/16" and an outer diameter of 1/8" was attached to the ends of the column. After a solution of 1 M NaOH was passed through the column for a few minutes to ensure the bed was settled, NCAW waste simulant, which was previously spiked with ^{89}Sr to give a total Sr concentration of 0.024 mg/l and measured for its activity on the scintillation counter, was pumped through. Every few hours, the volume of the collected solution was measured along with its activity until about 25% of the effluent's activity had broken through. The

breakthrough curve, shown in Figure 3.6, shows that at 50% breakthrough, (this point was extrapolated as the column tubing clogged up with waste precipitate at 24%), with a flow rate of <30 ml/hr, the material was predicted to be able to remove 3.18×10^{-3} meq Sr/g from of total of 5700 ml of NCAW.

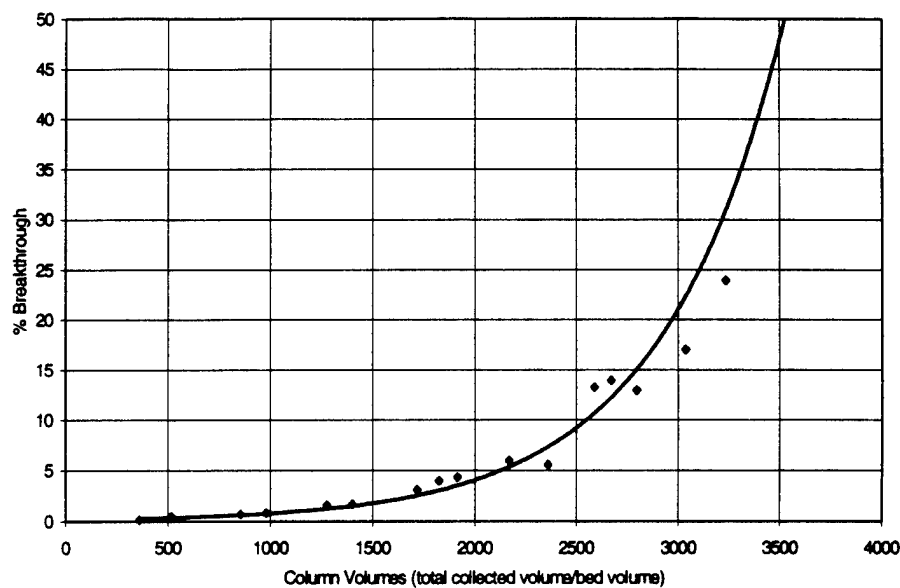


Figure 3.6. Sr column data for GMG-I-1 inorganic beads in NCAW simulant.

A similar column experiment was run using 0.2-0.5 mm GMG-I-1 beads which were made using 17% organic Polyacrylonitrile (PAN) binder by colleagues from the Czech Republic. At 50% breakthrough, these beads were able to exchange only $1.11 \times$

10^{-3} meq Sr/ml, which corresponded to about 3036 ml of waste simulant, at an equivalent flow rate, refer to Figure 3.7.

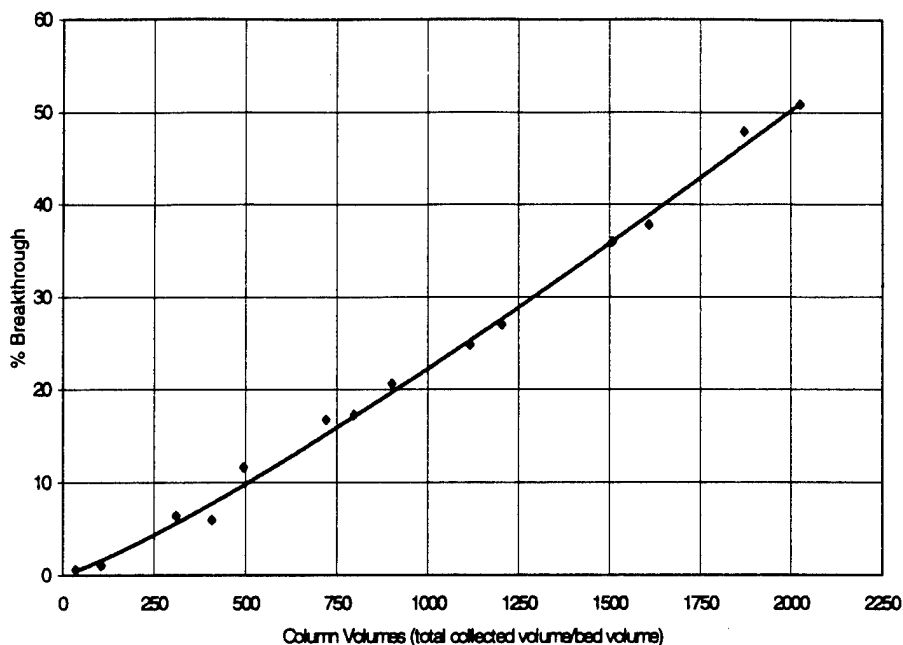


Figure 3.7. Sr column data for GMG-I-1 organic beads in NCAW simulant.

In order to understand this extreme difference in Sr capacities, batch test results from each type of beads in NCAW waste simulant were compared to K_d values from the powder form of GMG-I-1 in NCAW. Taking into account the % binders present, the inorganic beads gave a K_d of 83,200 and the organic beads gave Sr^{2+} K_d 's of 65,700, while the powder form gave a K_d of 250,100. This suggests that the inorganic binder aided in Sr^{2+} uptake as well as the fact that the organic binding material blocked the ion

exchange sites of the titanate more so than the inorganic binder. The combination of these actions caused the reduction in Sr^{2+} uptake in the organic bead column experiment.

In addition to batch tests, kinetic tests were performed on the inorganic beads in order to better understand the column results. In order to monitor the beads' rate of Sr exchange, 0.05g of GMG-I-1 inorganic beads were added to 20 ml of NCAW, which was spiked with ^{89}Sr to give a total Sr concentration of 0.4 mg/l, and shaken gently, while 0.05 ml samples were extracted at 1 minute intervals for 10 minutes, then at 30 minutes, 1 hour, 1.5, and 2 hours and tested for their activity. It was clear that the rate of exchange was slow as the results indicated that the K_d 's were still increasing after 1hr as seen in Figure 3.8.

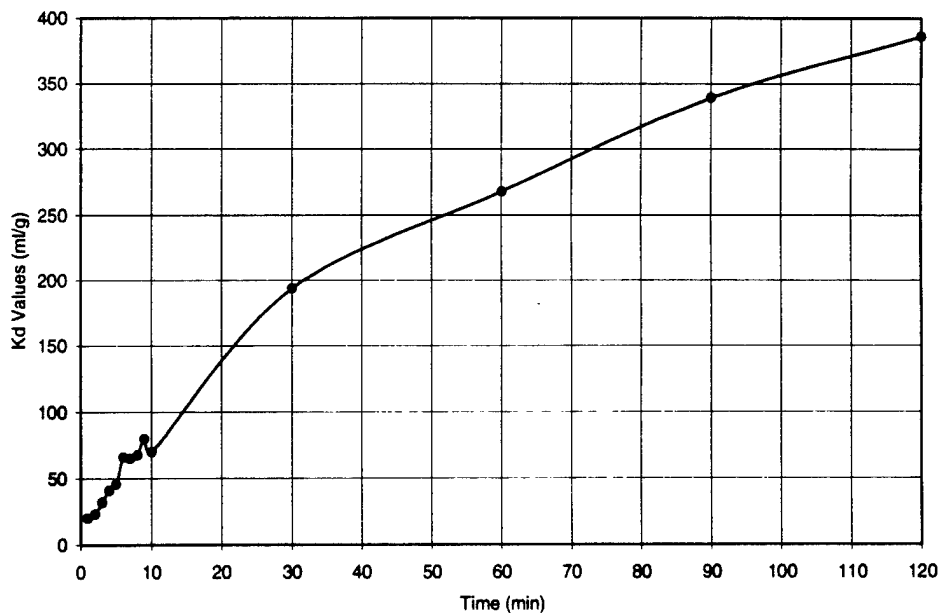


Figure 3.8. Sr exchange kinetic study on GMG-I-1 inorganic beads.

This indicates that with each minute longer the beads were in contact with the waste solution, more Sr^{2+} was exchanged. In effect, the larger the bed volume used in the column and the slower the flow rate, the longer solution would be in contact with the beads before it passed through, and the more effective the Sr exchange would be.

101SY Simulant. Due to the interesting results obtained from the 101SY tank waste simulant batch tests, column tests were run using this simulant, which was spiked with ^{89}Sr to give a total Sr concentration of 0.12 mg/l, with GMG-I-1 inorganic beads, following the same procedure as in the previous column experiments. By packing the beads in a 1 ml bed volume in a 0.7 x 4.0 cm Kontes Flex Column using Tygon tubing with inner and outer diameters of 0.0351" and 0.1031", respectively, the flow rate was slowed to 5 ml/hr to allow the beads to exchange approximately 4.34×10^{-4} meq Sr/g of beads at 50% breakthrough, refer to Figure 3.9.

In order to improve these results, a similar column experiment was run using inorganic beads made from GMG-I-59 which was the synthesis that incorporated all parameter variations. Although this sample was optimized for Sr^{2+} exchange in Metal/Sr solutions, it was not effective in this particular simulant as was evidenced by the removal of a mere 3.37×10^{-4} meq Sr/g of beads, refer to Figure 3.10.

Industrial Testing

Samples of GMG-I-1 have been sent to the Hanford Site to be tested in actual wastes. Thus far, the performance of this sample, along with other ion exchangers, has

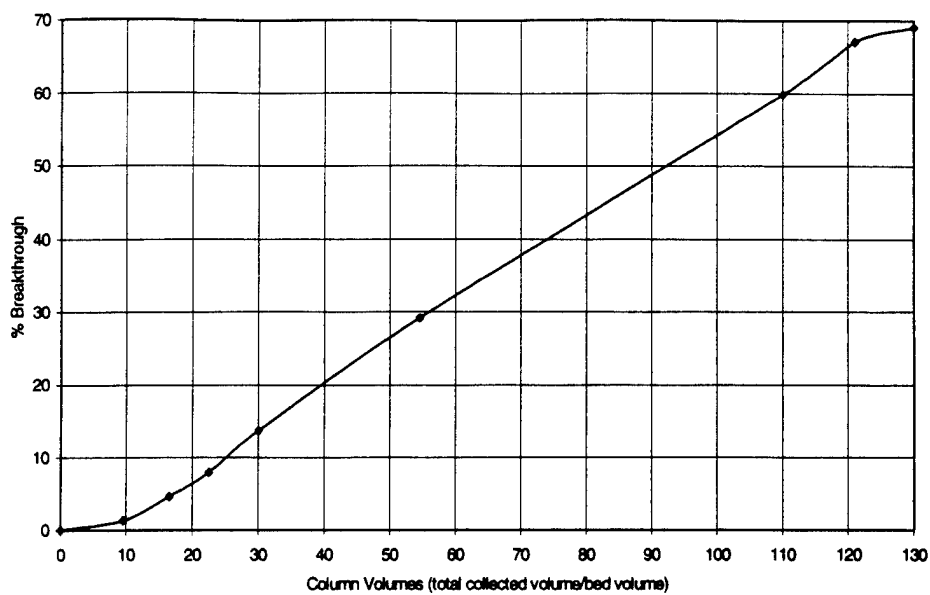


Figure 3.9. Sr column data for GMG-I-1 inorganic beads in 101SY simulant.

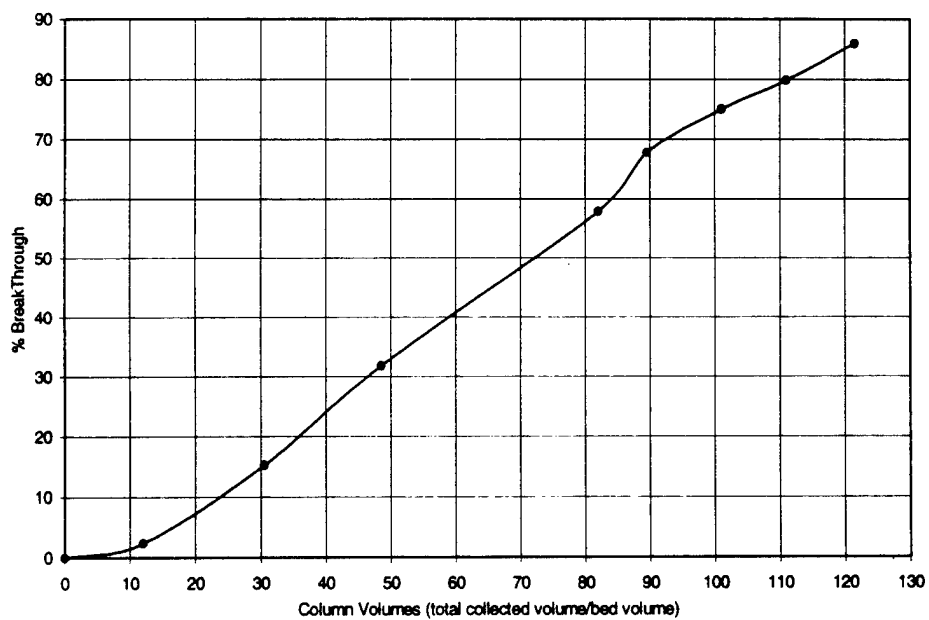


Figure 3.10. Sr column data for GMG-I-59 inorganic beads in 101SY simulant.

been assessed for KE-Basin water, which is where spent fuel rods have been stored. Over time, some of the rod claddings have cracked, causing radioactive materials, (such as ^{90}Sr), to leak into the water. The results presented in Table 3.5 show how GMG-I-1 compared with other exchangers in the removal of ^{90}Sr from this water. The best Sr^{2+} ion exchanger was the second pharmacosiderite sample with a K_d of 4.77×10^6 ; however, sample GMG-I-1 was a close second with a K_d of 1.83×10^6 . These data show that GMG-I-1 was more efficient at Sr removal than the Allied Signal scale-up of the nonatitanate and Sr-Treat, which gave a K_d 's of only 4.80×10^4 and 9.10×10^4 , respectively.³³ Further comparison testing of these materials in actual tank wastes is currently underway.

Table 3.5. Comparison of Sr K_d values for various exchangers in KE-Basin water using a volume : mass ratio of 10^4 .

		(ml/g)
Ion Exchanger	Sample #	Kd Values
IONSIV IE-911	99096810002	9.72E+04
Clinoptilolite	n/a	9.03E+04
K Co Hexacyanoferrate	2999-14	2.35E+04
Pharmacosiderite	E-B Pharm-1	6.44E+05
Sodium Biotite	8212-15D	6.96E+04
Sodium Biotite	8212-32A	4.89E+04
Na Nonatitanate (Allied Signal)	8212-152	4.80E+04
Cs-Treat	H58	2.17E+04
Sr-Treat	H18	9.10E+04
Pharmacosiderite	AIB-TS255	4.77E+06
Na Nonatitanate (TAMU)	GMG-I-1	1.83E+06

CHAPTER IV

CONCLUSIONS

Modification of the synthesis of sodium nonatitanate, where variations in the synthetic parameters, (heating time, oven temperature, Na:Ti mole ratio, heating method), were individually explored, has led to alteration of the material's ion exchange properties. It seemed that the less time the synthesis reactants were heated in the oven, or the lower the oven temperature, the less crystalline the titanate product was until a point was reached where the oven contact time was too short, (sample GMG-I-28, which excluded the hydrothermal bomb step), or where the temperature was too low, (sample GMG-I-22a, that was heated at 150°C), for the Na nonatitanate to form. In correlation with this reduced titanate crystallinity, an improvement in the material's ion exchange selectivity for Sr^{2+} in Na, Mg, Ca, and Ba/Sr solutions was observed. However, in the series where the heating method was altered, the least crystalline sample, GMG-I-27, that was prepared without the 3 hour preheating step, was not as selective for Sr^{2+} exchange as sample GMG-I-39 that was heated for 1 day and slowly cooled overnight. This indicates that in this case, GMG-I-27 may not have been structured enough for Sr^{2+} removal. Although the Na:Ti mole ratio variation series of experiments did not affect the crystallinity of the material, it seemed that the larger the ratio, the more selective the titanate product was for Sr^{2+} .

Throughout these synthesis variations, generally, Ca^{2+} ions posed the greatest competition to Sr^{2+} exchange due to their similar ionic sizes. However, the K_d results of some of the synthesis variations showed the greatest competition to be from Mg^{2+} ions.

The fact that Mg^{2+} is much smaller than Sr^{2+} leads to the possible conclusion that the synthesis variations altered the exchange sites of these samples in such a way to better accommodate Mg^{2+} exchange. However, it is difficult to say exactly what is happening as the poor crystallinity of these materials prevents the determination of a crystal structure.

Within this experimental set, the most effective sample for Sr^{2+} exchange in alkaline earth metal/Sr solutions came from the final synthesis which combined the most effective parameter changes from each variation series. These included using a 6.00 Na:Ti mole ratio with the 3 hour preheating step, the hydrothermal bomb step at 170°C for 2 days, and a final quick cooling of the bomb under the tap to quench the reaction. This synthesis was able to improve the original synthesis K_d values from a range of 360,700 to 43,700 in different concentrations of Na/Sr solutions to a range of 1,344,400 to 124,700, as shown in Table 3.1.

In another set of syntheses, the original Ti and Na reactants were replaced by other metals. The samples where Zr was used as the tetravalent metal and where KOH and CsOH were used as the base in the reaction proved to be ineffective for Sr^{2+} and Cs^+ ion exchange. In samples GMG-I-33 & 34, $\text{Sr}(\text{NO}_3)_2$ was added into the reaction mixture along with NaOH. This was done in order to produce a Sr nonatitanate which would retain the dimensions of the Sr^{2+} ions in the exchange sites after exchange of the Sr^{2+} ions for Na^+ ions. In essence, Sr^{2+} would act as a template to fashion the best exchange site for the amorphous nonatitanate, thereby creating a material with greater Sr^{2+} selectivity. However, a stable, non-exchangeable Sr titanate, SrTiO_3 , was produced

and although it could not be used for Sr^{2+} exchange, further tests revealed that this stable product could be formed upon heating a Sr exchanged Na nonatitanate, providing a safe means of storage for the spent exchangers.

The Sr exchange selectivities were examined for samples GMG-I-1 & 10a-d in NCAW waste simulant. The most effective Sr exchanger in this series was GMG-I-1 with a K_d of 250,100. In comparison with other ion exchangers such as Na titanosilicate and K titanosilicate pharmacosiderite, which, respectively, gave Sr K_d 's of 269,500 and 20,200 in NCAW, GMG-I-1 appears to be a rather competitive material.

Column tests performed on beads made out of GMG-I-1 using an inorganic binder in NCAW waste simulant showed that the material was able to exchange 3.18×10^{-3} meq Sr/g when using a 1.5 ml bed volume at a flow rate of <20 ml/hr. In actual industrial testing, the size of the bed volume would be much larger and the flow rate would be much slower which would increase the length of time the solution would be in contact with the exchanger, increasing the material's Sr uptake. Therefore, the Sr^{2+} uptake from this material is expected to increase during on site testing.

The original synthesis sample, GMG-I-1, was also tested for its Sr selectivity in 101SY waste simulant which contains Sr complexing agents. Although the K_d values for this material were low, 295 ml/g, they were competitive with other exchangers such as Na titanosilicate and K titanosilicate pharmacosiderite which gave K_d 's of 231 and 31, respectively. Column tests performed on this material in 101SY simulant showed the sample to be able to exchange 4.34×10^{-4} meq Sr/g. In order to improve these results, additional column tests were run on sample GMG-I-59 which was optimized for Sr^{2+}

uptake in Metal/Sr solutions. However, this material removed less Sr^{2+} , 3.37×10^{-4} meq Sr/g, than the previous sample. This shows that even though this material was optimized for Sr removal in Metal/Sr solutions, GMG-I-59 was not able to remove Sr^{2+} as efficiently from the chelating 101SY waste simulant.

Each titanate sample was tested for its Cs exchange selectivity in N-Springs groundwater simulant. Unfortunately, because of cesium's large ionic size, the materials could not efficiently exchange Cs^+ , as seen by the K_d 's of <1200 . However, sample GMG-I-24a, in which the exact 4:9 stoichiometric ratio was used, and sample GMG-I-43a1, in which CsOH was substituted for NaOH in the synthesis, produced K_d 's of 3740 and 5230, respectively. This indicates that these synthesis variations produced samples with exchange sites large enough to partially accommodate Cs^+ .

The work presented here provides a thorough investigation of the Sr^{2+} exchange selectivities in alkaline earth solutions for a variety of different sodium nonatitanates for which the synthesis variables were systematically changed. However, as seen with samples GMG-I-10a and GMG-I-59, which were optimized for Sr uptake in Metal/Sr solutions (but were not as efficient in simulated wastes), the synthesis variations may have altered the exchange sites so that Sr^{2+} ion exchange efficiency differs from one tank waste to another depending on the type and concentration of competing ions. Therefore it is necessary that additional tests are completed in the future where every nonatitanate sample produced in this work is tested for Sr^{2+} uptake in each type of tank waste in order to find the optimum material for each waste. Once it is determined which sample most efficiently removes Sr^{2+} from each tank waste simulant, these materials need to be tested

on the actual wastes, and compared with other leading ion exchangers. It is also hoped that in the future, a crystal structure of the nonatitanate can be determined in order to better understand exactly how the synthesis variations changed the material's structure so that predictions can be made of its Sr exchange efficiency in specific types of wastes.

REFERENCES

1. Bailey, R. A.; Clark, H. M.; Ferris, J. P.; Krause, S.; Strong, R. L. *Chemistry of the Environment*; Academic Press: New York, 1978.
2. Navratil, O.; Hala, J.; Kopunec, R.; Macesek, F.; Mikulaj, V.; Leseticky, L. *Nuclear Chemistry*; Ellis Horwood PTR Prentice Hall: New York, 1992.
3. Lumetta G. J.; Wagner, M. J.; Carlson, C. D. *Solv. Extr. & Ion Exch.* **1996**, *14*, 35-60.
4. Ahearne, J. F. *Physics Today.* **1997**, *50*, 24-29.
5. Crowley, K. D. *Physics Today.* **1997**, *50*, 32-39.
6. Winters, W. I.; Esch, R. A.; Welsh, T. L.; Wyse, E. J. "Tank Waste Remediation System Privatization Contractor Samples Low Activity Waste Envelope 'C' Tank 241-AN-107", HNF-SD-WM-DP-205, rev. 1, British Nuclear Fuels, March 1997.
7. Clearfield, A. In *Industrial Environmental Chemistry*; Sawyer, D. T.; Martell, A. E., Eds.; Plenum Press: New York, 1992; pp. 289-299.
8. Levi, B. G. *Physics Today.* **1992**, *45*, 17-21.
9. Kastenber, W. E.; Gratton, L. J. *Physics Today.* **1997**, *50*, 41-46.
10. North, D. W. *Physics Today.* **1997**, *50*, 48-54.
11. Chiarizia, R.; Ferraro, J. R.; D'Arcy, K. A.; Horwitz, E. P. *Solv. Extr. & Ion Exch.* **1995**, *13*, 1063-1082.
12. Horwitz, E. P.; Dietz, M. L.; Fisher, D. E. *Solv. Extr. & Ion Exch.* **1991**, *9*, 1-25.
13. Harjula, R.; Lehto, J. *Nucl. and Chem. Waste Mgt.* **1986**, *6*, 133-137.

14. Collins, E. D.; Campbell, D. O.; King, L. J.; Knauer, J. B.; Wallace, R. M.
“Evaluation of Zeolite Mixtures for Decontaminating High-Activity Level Water at the 3 Mile Island Unit.2 Nuclear Power Station”, In *Inorganic Ion Exchangers & Adsorbents for Chemical Processing in the Nuclear Fuel Cycle*, International Atomic Energy Agency, Vienna; 1985.
15. Kanno, T.; Mimura, H. “Ion Exchange Properties of Zeolites and Their Application to Processing of High-Level Liquid Waste”, In *Inorganic Ion Exchangers & Adsorbents for Chemical Processing in the Nuclear Fuel Cycle*, International Atomic Energy Agency, Vienna; 1985.
16. Poojary, D. M.; Cahill, R. A.; Clearfield, A. *Chem. Mater.* **1994**, *6*, 2364-2368.
17. Bortun, A. I.; Bortun, L. N.; Clearfield, A. *Solv. Extr. & Ion Exch.* **1996**, *14*, 341-354.
18. Behrens, E. A.; Poojary, D. M.; Clearfield, A. *Chem Mater.* **1996**, *8*, 1236-1244.
19. Harjula, R.; Lehto, J.; Saarinen, L.; Paajanen, A.; Tusa, E. “CsTreat - Superior Ion Exchange Material for the Removal of Radioactive Cs from Nuclear Waste Effluents”, Waste Management '96 Conference, Tucson, Arizona; 1996.
20. Harjula, R.; Lehto, J.; Brodtkin, L.; Tusa, E. “CsTreat - Highly Efficient Ion Exchange Media for the Treatment of Cs Bearing Waste Waters”, EPRI International Low-Level Waste Conference, Providence, Rhode Island; 1997.
21. Lynch, R. W.; Dosch, R. G.; Kenna, B. T.; Johnstone, J. K.; Nowak, E. J. “The Sandia Solidification Process - A Broad Range Aqueous Waste Solidification

- Method”, In *Management of Radioactive Wastes from the Nuclear Fuel Cycle*, International Atomic Energy Agency, Vienna; 1976.
22. Izawa, H.; Kikkawa, S.; Koizumi, M. *J. Phys. Chem.* **1982**, *86*, 5023-5026.
23. Sasaki, T.; Watanabe, M.; Komatsu, Y.; Fujiki, Y. *Inorg. Chem.* **1985**, *24*, 2265-2271.
24. Sasaki, T.; Komatsu, Y.; Fujiki, Y. *Chem. Lett.* **1981**, *7*, 957-960.
25. Clearfield, A.; Lehto, J. *J. Solid State Chem.* **1988**, *73*, 98-106.
26. Lehto, J.; Harjula, R.; Girard, A. *J. Chem. Soc. Dalton Trans.* **1989**, *1*, 101-103.
27. Lehto, J.; Heinonen, O. J.; Miettinen, J. K. *Radiochem. Radioanal. Let.* **1981**, *46*, 381-388.
28. Cahill, R. A. Ph.D. Dissertation, Texas A&M University, May 1996.
29. Wadsley, A. D. *Acta Cryst.* **1964**, *17*, 623-628.
30. Rebbah, H.; Desgardin, G.; Raveau, B. *J. Solid State Chem.* **1980**, *31*, 321-328.
31. Anthony, R. G.; Dosch, R. G.; Philip, C. V. “Novel Silico-Titanates and Their Methods of Making and Using”, World Patent, WO 94/19277; 1994.
32. Behrens, E. A.; Sylvester, P.; Graziano, G.; Clearfield, A. In *Science and Technology for Disposal of Radioactive Tank Wastes*; Lombardo, N. J.; Schulz, W. W., Eds.; Plenum Publishing Corporation: New York, in press.
33. Brown, G. N.; Bontha, J. R.; Carson, K. J.; Elovich, R. J.; DesChane, J. R. Pacific Northwest National Laboratory, Richland, Washington; 1997, personal communication.

APPENDIX A

Table A.1. K_d values for GMG-I-1 in Na/Mg, Na/Ca, Na/Sr, and Na/Ba solutions.

mol/l	GMG-I-1 K_d Values (ml/g)			
[Na]	Mg	Ca	Sr	Ba
0.001	53052	32569	107061	14274
0.01	53842	20346	360658	8869
0.1	49901	16689	325035	2230
1	13487	14482	43726	269

Table A.2. K_d values for the heating time variation series in Na/Sr solutions.

mol/l	K_d Values (ml/g)				
[Na]	GMG-I-1	GMG-I-10a	GMG-I-10b	GMG-I-10c	GMG-I-10d
0.001	107061	141152	246432	242362	145245
0.01	360658	816790	195112	197591	160312
0.1	325035	1216497	168905	138607	85663
1	43726	53953	40470	23110	14770

Table A.3. K_d values for the heating time variation series in Mg/Sr solutions.

mol/l	K_d Values (ml/g)				
[Mg]	GMG-I-1	GMG-I-10a	GMG-I-10b	GMG-I-10c	GMG-I-10d
0.001	134616	113270	166836	194842	186318
0.01	229228	134037	38203	40865	37485
0.1	19528	13242	182	1507	636
1	1090	896	30	14	4

Table A.4. K_d values for the heating time variation series in Ca/Sr solutions.

mol/l	Kd Values (ml/g)				
[Ca]	GMG-I-1	GMG-I-10a	GMG-I-10b	GMG-I-10c	GMG-I-10d
0.001	84780	204946	105223	45618	67546
0.01	65766	77618	28292	67218	26142
0.1	32	30	39	30	9
1	6	3	4	2	0

Table A.5. K_d values for the heating time variation series in Ba/Sr solutions.

mol/l	Kd Values (ml/g)				
[Ba]	GMG-I-1	GMG-I-10a	GMG-I-10b	GMG-I-10c	GMG-I-10d
0.001	202164	127380	96677	155404	70416
0.01	109909	158699	142034	309938	129790
0.1	166	147	55	38	21

Table A.6. K_d values for the oven temperature variation series in Na/Sr solutions.

mol/l	Kd Values (ml/g)		
[Na]	GMG-I-22a	GMG-I-22b	GMG-I-1
0.001	125817	854175	107061
0.01	16921	1059431	360658
0.1	337653	774366	325035
1	38833	75579	43726

Table A.7. K_d values for the oven temperature variation series in Mg/Sr solutions.

mol/l	Kd Values (ml/g)		
[Mg]	GMG-I-22a	GMG-I-22b	GMG-I-1
0.001	165902	470538	134616
0.01	91612	108249	229228
0.1	816	1773	19528
1	54	77	1090

Table A.8. K_d values for the oven temperature variation series in Ca/Sr solutions.

mol/l	Kd Values (ml/g)		
[Ca]	GMG-I-22a	GMG-I-22b	GMG-I-1
0.001	428820	1191161	84780
0.01	129864	123673	65766
0.1	55	60	32
1	7	5	6

Table A.9. K_d values for the oven temperature variation series in Ba/Sr solutions.

mol/l	Kd Values (ml/g)		
[Ba]	GMG-I-22a	GMG-I-22b	GMG-I-1
0.001	312187	634156	202164
0.01	175488	300304	109909
0.1	138	190	166

Table A.10. K_d values for the Na:Ti mole ratio variation series in Na/Sr solutions.

mol/l	Kd Values (ml/g)			
[Na]	GMG-I-24a	GMG-I-24b	GMG-I-1	GMG-I-24c
0.001	11769	61348	107061	112335
0.01	112396	470220	360658	459337
0.1	1010511	450128	325035	1517518
1	7047	82287	43726	68692

Table A.11. K_d values for the Na:Ti mole ratio variation series in Mg/Sr solutions.

mol/l	Kd Values (ml/g)			
[Mg]	GMG-I-24a	GMG-I-24b	GMG-I-1	GMG-I-24c
0.001	23679	163629	134616	275075
0.01	72585	286875	229228	138807
0.1	4987	2501	19528	6295
1	366	133	1090	283

Table A.12. K_d values for the Na:Ti mole ratio variation series in Ca/Sr solutions.

mol/l	Kd Values (ml/g)			
[Ca]	GMG-I-24a	GMG-I-24b	GMG-I-1	GMG-I-24c
0.001	4820	66341	84780	963318
0.01	12432	156604	65766	123430
0.1	41	43	32	40
1	8	6	6	5

Table A.13. K_d values for the Na:Ti mole ratio variation series in Ba/Sr solutions.

mol/l	Kd Values (ml/g)			
[Ba]	GMG-I-24a	GMG-I-24b	GMG-I-1	GMG-I-24c
0.001	8303	357052	202164	1123173
0.01	22837	503023	109909	156477
0.1	31	201	166	173

Table A.14. K_d values for the heating method variation series in Na/Sr solutions.

mol/l	Kd Values (ml/g)			
[Na]	GMG-I-27	GMG-I-28	GMG-I-1	GMG-I-39
0.001	1182966	39090	107061	384231
0.01	470220	195561	360658	748408
0.1	47956	28488	325035	390798
1	28107	30277	43726	42382

Table A.15. K_d values for the heating method variation series in Mg/Sr solutions.

mol/l	Kd Values (ml/g)			
[Mg]	GMG-I-27	GMG-I-28	GMG-I-1	GMG-I-39
0.001	335635	91897	134616	711955
0.01	61235	31631	229228	108819
0.1	768	2278	19528	7728
1	67	120	1090	398

Table A.16. K_d values for the heating method variation series in Ca/Sr solutions.

mol/l	Kd Values (ml/g)			
[Ca]	GMG-I-27	GMG-I-28	GMG-I-1	GMG-I-39
0.001	465765	212327	84780	657664
0.01	62189	117406	65766	104636
0.1	36	10	32	34
1	1	1	6	0.1

Table A.17. K_d values for the heating method variation series in Ba/Sr solutions.

mol/l	Kd Values (ml/g)			
[Ba]	GMG-I-27	GMG-I-28	GMG-I-1	GMG-I-39
0.001	237941	83514	202164	537432
0.01	23208	91439	109909	304510
0.1	125	23	166	158

VITA

Gina Marie Graziano

179 Ames Street

Hackensack, NJ 07601

Education:

Master of Science from Texas A&M University, College Station, TX. Chair of Advisory Committee: Dr. Abraham Clearfield. Major subject: Chemistry. August 1996 through May 1998.

Bachelor of Science from Rensselaer Polytechnic Institute, Troy, NY. Major subject: Chemistry. Concurrently received a commission as a Second Lieutenant in the United States Air Force. August 1992 through May 1996.